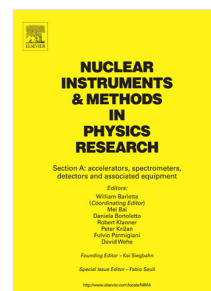


## Accepted Manuscript

An event-triggered coincidence algorithm for fast-neutron multiplicity assay corrected for cross-talk and photon breakthrough

R. Sarwar, V. Astromskas, C.H. Zimmerman, G. Nutter, A.T. Simone, S. Croft, M. J. Joyce



PII: S0168-9002(18)30787-3  
DOI: <https://doi.org/10.1016/j.nima.2018.06.056>  
Reference: NIMA 60917

To appear in: *Nuclear Inst. and Methods in Physics Research, A*

Received date: 11 February 2018  
Revised date: 26 May 2018  
Accepted date: 20 June 2018

Please cite this article as: R. Sarwar, V. Astromskas, C.H. Zimmerman, G. Nutter, A.T. Simone, S. Croft, M.J. Joyce, An event-triggered coincidence algorithm for fast-neutron multiplicity assay corrected for cross-talk and photon breakthrough, *Nuclear Inst. and Methods in Physics Research, A* (2018), <https://doi.org/10.1016/j.nima.2018.06.056>

This is a PDF file of an unedited manuscript that has been accepted for publication. As a service to our customers we are providing this early version of the manuscript. The manuscript will undergo copyediting, typesetting, and review of the resulting proof before it is published in its final form. Please note that during the production process errors may be discovered which could affect the content, and all legal disclaimers that apply to the journal pertain.

\*Manuscript

[Click here to view linked References](#)

# An event-triggered coincidence algorithm for fast-neutron multiplicity assay corrected for cross-talk and photon breakthrough

R. Sarwar<sup>1</sup>, V. Astromskas<sup>1</sup>, C. H. Zimmerman<sup>3</sup>, G. Nutter<sup>2</sup>, A. T. Simone<sup>2</sup>, S. Croft<sup>2</sup> and M. J. Joyce<sup>1,\*</sup>

<sup>1</sup>Department of Engineering, Lancaster University, Lancaster, LA1 4YW, UK.

<sup>2</sup>Oak Ridge National Laboratory, PO Box 2008 MS-6335, Oak Ridge TN 37831, USA.

<sup>3</sup>Central Laboratory, National Nuclear Laboratory, Sellafield, CA20 1PG, UK.

\*Corresponding author: [m.joyce@lancaster.ac.uk](mailto:m.joyce@lancaster.ac.uk)

## Abstract

A model quantifying detector cross-talk and the misidentification of events in fast neutron coincidence distributions is described. This is demonstrated for two experimental arrangements comprising rings of 8 and 15 organic liquid scintillation detectors. Correction terms developed as part of this model are tested with <sup>252</sup>Cf and a relationship is developed between the <sup>235</sup>U enrichment of U<sub>3</sub>O<sub>8</sub> and the order of correlated, fast neutron multiplets induced by an americium-lithium source. The model is also supported by Geant4 simulations. The results suggest that a typical assay, for experimental arrangements that are similar to the examples investigated in this research, will exhibit cross-talk for less than 1% of all detected fast neutrons but, if not accounted for, this can bias the numerical analysis by a margin of 10% and 35% in second- and third-order coincidences (i.e. couplet and triplet counts), respectively. Further, for the case of <sup>252</sup>Cf, it is shown that a relatively low proportion of 4% breakthrough by  $\gamma$  rays (that is, photons misidentified as neutrons by the pulse-shape discrimination process) can lead to an erroneous increase of 20% in total neutron counts in the assay of a mixed-field, in this case of <sup>252</sup>Cf. These findings will help direct the developments needed to enable organic scintillation detectors with pulse shape discriminators to be applied reliably to nuclear safeguards and non-proliferation verification tasks.

Keywords: neutron, scintillator, multiplicity, cross-talk, breakthrough, gate fraction.

## 1. Introduction

In nuclear safeguards, fissile material assay is used routinely as one of a number of procedures to ensure that nuclear materials are properly accounted for and not misused. An established technique to this end is neutron multiplicity counting [1, 2]. Historically, this method has been deployed using detector systems based on  $^3\text{He}$  gas for the detection of time-correlated, thermalised neutrons emitted from spontaneous fission (SF) and induced fission (IF). Whilst essentially immune to  $\gamma$  radiation and having high detection efficiencies,  $^3\text{He}$ -filled proportional counters have the drawback that their sensitivity is optimised for neutrons with energies in the thermal domain. Therefore, the detection apparatus is often arranged to incorporate a stage that is dedicated to the thermalisation of the fast neutrons prior to detection. In addition to reducing the energy of the neutrons, this also increases the source-to-detector time-of-flight due to the time taken for the neutrons to pass through the intermediate stage in which elastic scattering is encouraged to slow the neutrons down to thermal energies.

The implication of this is two-fold in so far as multiplicity and temporal analyses are concerned: (i) the coincidence window needed is substantially wider (that is, of the order of 40-50 ns) [3] compared to the typical time taken for the fission-correlated fast neutron field to die away (typically 20-25 ns), thus influencing acquisition time and statistical uncertainty; and (ii) information on the incident neutron energy is effectively lost in this process, eliminating the prospect of this being exploited for complementary, analytical purposes. Since the rise and fall (the latter being the prompt neutron die-away) of the neutron population in a fission chain can be due to either SF, ( $\alpha$ , n) reactions or scattering, and the timing of these different distributions cannot be discerned comprehensively where intermediate thermalisation is necessary, some aspects of the change in the neutron population cannot be determined fully with  $^3\text{He}$  detectors.

Amongst the earliest reports of fast-neutron multiplicity counting based on the use of organic scintillators in an unmoderated environment is that of Wachter et al. [4]. This highlighted the key potential benefits of fast neutron methods, such as multiplicity sensitivity beyond coincident events and significantly-reduced levels of accidentals, over thermal assays. However, it also highlighted the need to correct for: cross-talk, i.e., a chance coincidence where a single neutron can scatter from one

scintillation detector to another depositing energy in both, therefore provoking a correlated combination of several events between detector elements (referred to in that work as *multiple-order scattering*); pileup; and the mis-assignment of photons as neutrons (hereafter referred to as *photon breakthrough*). Wachter et al. highlighted the particular significance of these corrections for the case of materials exhibiting high ( $\alpha, n$ ) yields (relative to fission neutrons) in reducing significant discrepancies in mass assessments that might arise otherwise.

Subsequently, preliminary Monte Carlo studies of system designs taking advantage of liquid scintillator-based, fast-neutron assay systems were reported [5]. These designs adopted thermal neutron coincidence counting auto-correlation techniques that were modified to address the differences in the physics between the two detector systems. Since then, several related counter developments and concepts [6] have been reported using active neutron interrogation [7], and have included further modelling and simulation studies [8–10].

Despite having lower detection efficiencies, organic liquid scintillation detectors can have an advantage in environments associated with items that emit radiation at relatively high rates where chance coincidences can dominate, because they have significantly shorter coincidence gate width requirements, as shown in previous studies [11]. The absence of a thermalisation stage enables coincidence gate-widths of the order of 25 ns to be used, for both neutron and  $\gamma$ -triggered coincidence distributions. This has been accomplished, as described in section 2a of this work, using the Hybrid Instruments Ltd. MFAX analyser [12], coupled with an off-the-shelf Field-Programmable Gate Array (FPGA), to undertake multiplicity and temporal analysis in real-time, i.e. without post-processing. This approach used a novel algorithm that works with the size of event clusters in contrast to the traditional approach which is based on analysis of the reduced factorial moments. The shorter coincidence gate-width results in a significant reduction in accidental counts to give reduced levels of uncertainty and increased sensitivity to higher orders of net multiplicity.

However, challenges remain due to two principal disadvantages of organic scintillation materials. Firstly, the relatively high sensitivity of organic scintillators to photons in contrast with that of  $^3\text{He}$  detectors, coupled with shortfalls in the event discrimination mechanism, can lead to 3-5% of photons (depending on the pulse-shape discrimination (PSD) algorithm being used) being

misclassified as neutrons as per the photon breakthrough phenomenon defined earlier. This can have a disproportionate impact on neutron count rates as the ratio between number of neutron and photons emitted from either spontaneous or induced fission is typically of the order of 1:10, for the case of  $^{252}\text{Cf}$ , for example. Secondly, cross-talk events arising as a result of a single neutron or photon scattering from one detector to another, thus triggering multiple detectors, can masquerade as correlated multiplets. If a correction for these effects is not made then the assay can be undermined as per, for example, the observations of Wachter et al. [4] referred to earlier. Engineering challenges such as temperature stabilization, automated setup and so forth for a complex array also exist, but can be overcome by design. Whilst it is possible to configure the PSD algorithm to have very high detector cut-offs in order to operate the detector array in a region where these phenomena are not a hindrance, such an approach is not ideal as it comes at the expense of reduced neutron counts, i.e. reduced neutron efficiency.

Several attempts have been made to address these issues, both experimentally [13, 14] and analytically [15, 16, 17]. Perhaps most simply, coincident events in adjacent detectors might be discarded (usually by the acquisition firmware or in post-processing) on the basis that cross-talk is most likely to occur between neighbouring detectors; indeed, this is implemented in some commercially-available systems by default. However, this is less than ideal as it might lead to an over-correction given the scenario that bona fide correlated events detected in neighbouring scintillators are also removed. This is especially relevant given the typical, polarised angular correlation between fission neutrons, particularly when tested with isotopes with high values of  $\bar{\nu}$ , such as  $^{252}\text{Cf}$ , where a real correlation in neighbouring detectors might be plausible. Furthermore, for safeguards applications, 2D arrangements of detectors are usually simpler to configure and use than 3D arrangements but detector-detector distances of the former cannot be optimised to minimise cross-talk as easily as in the latter, thus motivating the need for the correction developed here.

The characteristics of neutron cross-talk have been examined before [15] using a  $^{252}\text{Cf}$  source, however the results were akin to the cosine distribution consistent with the angular distribution of the source rather than the anticipated isotropic distribution anticipated for cross-talk. The analytical

methods suggested by Li et al. [16] and Shin et al. [17] address this problem in a complicated manner using a reduced factorial distribution from a shift register based algorithm.

In this paper, we introduce a correction model based on a relatively simple, event-cluster algorithm using a balance equation to address both detector cross-talk and event mischaracterization. The coefficients for this model can be derived either experimentally or through simulations. In Section 2, a description of the event-triggered coincidence algorithm and the techniques used for the simulation of the coefficients and validation of the model are presented. Section 3 outlines the experimental techniques with which the approach has been tested, the correction models developed as part of this research are described in Section 4 and the validation of these models is discussed in Section 5. Section 6 summarises the conclusions from the research.

## 2. Algorithms

### (a) *Event-triggered Coincidence Algorithm*

Coincidence counting based on thermal neutrons tends to have relatively large emission-to-detection times in the range 1-100  $\mu$ s, due to the time necessary for thermalisation. This usually limits a one-shot coincidence algorithm [2] to low count rates. Hence, most assessments based on the detection of thermal neutrons use a coincidence algorithm based on a shift-register [2] to avoid dead time corrections. In the shift-register method, triggers are issued for every incoming event and each starts a new counting window, as illustrated in Figure 1a. This yields a reduced factorial moment distribution of incoming neutron events; this approach is accepted universally for fissile materials assay in nuclear safeguards. The every-event triggered coincidence distribution is commonly referred to as a multiplicity histogram, and the orders of “multiplicity” are referred to as singles, doubles, triples, quadruples, etc.; these being the 1<sup>st</sup>, 2<sup>nd</sup>, 3<sup>rd</sup>, 4<sup>th</sup>, etc. net reduced factorial moments on the pulse train.

However, mixed-field analysers used with liquid scintillators have significantly-reduced electronic dead-time, being capable of processing up to 3 million events per second [12]. Moreover, because thermalisation is unnecessary, both the emission-to-detection time and the signal duration are

small, i.e., both of the order of several tens of nanoseconds. Hence, the use of an *event-triggered coincidence algorithm* is viable in a fast neutron assay. In this method, when a neutron is first detected such that no prior events have occurred constituting a trigger, the system will issue a trigger. This opens a user-defined prompt gate for the prompt coincidence counter and disables the trigger mechanism. During this window, the algorithm scans for incoming photon and/or neutron events and these are counted. Following the end of the prompt gate, the system is idled for 150 ns and then a delayed gate is opened to assess the accidental coincidence distribution. At the end of each of the two windows, a signal is issued which increments the corresponding foreground and background coincidence distributions and re-activates the trigger mechanism. Hence, in the event sequence illustrated by way of example in Figure 1b, only the 1<sup>st</sup>, 5<sup>th</sup> and 6<sup>th</sup> triggers are issued, as this is when the trigger architecture is sensitive to incoming events. This prevents the same neutron event to be counted multiple times and, as such, the resulting distribution corresponds to the number of neutrons in a cluster in the neutron event train. This number distribution, referred to hereafter as the event-triggered coincidence distribution, can be converted easily to the reduced factorial moment distribution in order to apply existing analytical models [2] whilst having the benefit of being able to infer the order of coincidence directly, i.e., via the size of the clusters/bursts, without the need to carry out further mathematical analysis. The order of coincidence for the event-triggered distribution is inferred by the terms singlets, couplets, triplets, quarts, etc. in this work to differentiate it from the terminology associated with the traditional approach.

(b) *Geant4 model*

Monte Carlo simulations were used to determine the coefficients of the two models since it was not possible to determine these through experimentation, and they were also used to validate the models. In this sub-section, the details of the simulations are presented.

To model fission, the currently-available, general-purpose Monte Carlo codes (MCNP/X [18, 19], TART [20], Geant4 [21], etc.) employ an average fission model, that is, using uncorrelated fission neutrons and photons sampled from the same probability density function rather than those derived from a collection of individual fission processes. This is satisfactory for the calculation of

average quantities such as flux, energy deposition and multiplication. However, it is not ideal for an event-by-event analysis needed in materials assay.

MCNPX-PoliMi [22] includes the angular correlations of fission neutrons based on the assumption that the  $^{252}\text{Cf}$  spontaneous fission distribution can be employed for all fissionable nuclides. A more recent option introduced for the treatment of fission events, which utilizes the Lawrence Livermore National Laboratory (LLNL) fission library in MCNPX2.7.0 [23, 24], features time-correlated sampling of photons from neutron-induced fission, photo-fission and spontaneous fission. A disadvantage of these approaches is that they cannot simulate optical photons directly; rather they use an empirical formula for post-processing scripts to convert energy deposited in the detector (due to scattering of particles) to scintillation light output. Consequently, they do not take some of the optical properties of the detector into account and do not simulate the effect of light readout devices on the detector response.

Although Geant4 is able to model the scintillation process, it does not support correlated neutrons in isolation. However, it is possible to use the Fission Reaction Event Yield Algorithm (FREYA) [24] developed by LLNL to model correlations between neutron multiplicity, energy and angles, and energy sharing between neutrons and photons following a fission event within the particle generator inside Geant4, thereby combining the best of both worlds. Therefore, Geant4.10.3 was used in this research.

To take account of the corresponding transport physics, a custom physics list based on the Geant4 distributed QGSP BIC HP physics list was created. The neutron high-precision (HP) data transport model was used with the G4NDL4.5 neutron data library and thermal cross sections were derived largely from the ENDF/B-VII data library. The standard electromagnetic model was used for photons. The optical response from a scintillation detector was modelled with G4OpticalPhysics. Scintillation was done based upon the particle type, i.e., electron and proton. The scintillation yields from electrons and protons are plotted in Figure 2a [25, 26]. This methodology also accounts for light being produced, taking into account the quantum efficiency of the photomultiplier tubes (PMTs). Figure 2b illustrates the detector responses to photons from a  $^{137}\text{Cs}$  source. A complete validation of the neutron response using a similar method was done by Hartwig and Gumplinger [27].

### 3. Experimental methods

In this research organic liquid scintillation detectors of type VS-1105-21 (Scionix, Netherlands) have been used, comprising a scintillant volume of dimensions 100 mm × 100 mm × 120 mm filled with EJ-309 scintillant (Eljen Technology, Sweetwater, TX). Each has a PMT of type 9821 FLB (ADIT Electron Tubes, Sweetwater, TX). To discern whether a detection trigger is due to a fast neutron or photon, 4 quad-channel, real-time mixed-field-analysers (MFA) [28] were used which process inputs from up to 16 detectors, concurrently. The MFA integrates multichannel processing into a single, self-contained, portable unit driven by the same clock of 250 MHz and enables real-time coincidence processing of logic signals for input to a subsequent multiplicity register. The TTL signals from the MFA were routed to a field-programmable gate array (FPGA) development kit, via a 40-pin General Purpose Input/Output (GPIO) interface for carrying out multiplicity analysis. All detectors had a cut-off at approximately 200 keV electron equivalent. The size of the gate-width was set at 25 ns in accordance with preparatory measurements.

Both experiments described in this paper were conducted at Oak Ridge National Laboratory, TN, with a  $^{252}\text{Cf}$  source (for correlated neutrons), four americium-lithium (AmLi) sources (for uncorrelated neutrons) and a  $^{137}\text{Cs}$  source (for uncorrelated photons), in turn. The  $^{252}\text{Cf}$  source used in this case yields approximately  $3.32 \times 10^5$  fast neutrons per second from SF into  $4\pi$ , while the AmLi source emits approximately  $1.69 \times 10^5$  fast, uncorrelated neutrons per second from ( $\alpha$ , n) reactions. The duration of each experiment was adjusted to ensure less than 2.5% uncertainty for couplets events. During each experiment, both the count rates and the coincidence distribution (both foreground and background) were recorded.

Two detector arrangements were used in this research: the first comprised 8 detectors and the second 15 detectors. Each arrangement formed a ring located on an aluminium table, with the table 1 m from the floor and the sources positioned at the centre of the detectors. These are shown schematically in Figures 3a and 3b, with a photograph of the 15-detector arrangement given in Figure 3d. The distance from the source to the face of the detector was 20.5 cm and 26.25 cm for the 8- and 15-detector set-ups, respectively. This resulted in a corresponding angular separation between

neighbouring detectors of  $45^\circ$  and  $24^\circ$  for the 8- and 15-detector set-ups, respectively. Each of the detectors were placed on top of a 3.8 cm metal support to increase the clearance between them and the table, and a thin lead shield of 0.4 cm thickness was placed between the detectors and the source to reduce the low-energy photon flux when the neutron field was being measured. The sources were also lifted 8.5 cm from the table to align them with the horizontal axis of the detectors via aluminium supports, allowing for the thickness of the source holder.

In addition to the source-based arrangements described above, further experiments were conducted using nine standard  $\text{U}_3\text{O}_8$  canisters with radius 4 cm and height 8.9 cm. For these experiments, five of the canisters contained 200 g of  $\text{U}_3\text{O}_8$  powder with wt. %  $^{235}\text{U}$  enrichments of  $(0.3166 \pm 0.0002)$ ,  $(0.7119 \pm 0.005)$ ,  $(1.9420 \pm 0.0014)$ ,  $(2.9492 \pm 0.0021)$  and  $(4.4632 \pm 0.0032)$ , while three contained  $(229.99 \pm 0.1)$  g of  $\text{U}_3\text{O}_8$  with wt. %  $^{235}\text{U}$  enrichments of  $(20.31 \pm 0.02)$ ,  $(52.80 \pm 0.04)$  and  $(93.23 \pm 0.01)$ . These canisters were placed at the centre of the detector arrangements described above with a 2-cm thick polyethylene disk of 4.3 cm radius placed on top of them, on which an AmLi source was placed to provide the interrogating neutrons. This set of  $\text{U}_3\text{O}_8$  samples was investigated using the two configurations mentioned above, as well as the “castle” configuration depicted in Figure 3c.

#### 4. Models

##### (a) *Cross-talk:*

As highlighted above in Section 1, cross-talk occurs when a single neutron, detected first in one scintillator, is then scattered and detected in a second. This yields a second count which, if it occurs within the time window that is used to discriminate time-correlated neutrons from those that are not, can be mistaken as being the second event of a correlated pair; hence a singlet might appear to be a couplet as a result. Higher-order cross-talk events are plausible in the event of subsequent scatters that occur within the time gate. For clarity, one singlet that manifests as a couplet is referred to as *first-order cross-talk*, while a singlet appearing as a triplet is referred to as *second-order cross-talk*. If a

correction for these is not made, potentially-significant errors can result from singlet events being mis-assigned as correlated events in this way.

Using data from the Geant4 simulations described above, Figure 4a illustrates the probability of a cross-talk event taking place for the 15-detector set-up, based on 5 MeV neutrons from a mono-energetic beam subject to a variety of cut-off energies as a function of angle relative to the position of the detector stimulated by the first event. This simulation, along with others considered in this paper, was conducted with 1 million particles from a mono-energetic neutron or photon source. The particles were emitted from the centre of each detector arrangement with a fixed directional vector towards the top-most detector. In line with expectations, the probability of cross-talk between detectors is highest when the detectors involved in the event are nearest to one another with a small scattering angle relative to other scenarios. The contribution from cross-talk is negligible at angles greater than  $\sim 45^\circ$ . The potential for 2.2 MeV  $\gamma$  rays that arise from neutron capture on hydrogen to be treated as unresolved secondary particles in the simulations and tallied as neutrons has been removed by isolating them as photons and removing them from the tally. Experimentally, such events would be discarded by PSD, notwithstanding the possibility of their being misclassified although this scenario is not considered further in this paper.

Figure 4b shows the detector response as a function of the time that elapses between the primary detection and the detection of a cross-talk scatter event for neutrons in any of the detectors with energies of 1, 2, 3.5 and 5 MeV, and a cut-off energy of 200 keV. This demonstrates that cross-talk takes place in the range 5-to-40 ns for all cases, and most significantly for neutron energies 2, 3.5 and 5 MeV between 5 ns and 20 ns. Hence, it is desirable to correct for the excess activity that arises due to cross-talk. Further, based on the dependencies of the data presented in Figures 4a and 4b, it can be concluded that the cross-talk factor is a complicated function of the *geometry*, (that is the solid angles subtended by source-to-detector and by detector-to-detector), *detector cut-off*, *coincidence gate width* and *incident neutron energy*.

When a cross-talk event takes place, it can influence the coincidence distribution in two ways: (i) the singlet bin loses one count (referred to as *updraft*) and (ii) the couplet and potentially the

higher-order bins gain one count (referred to as *downdraft*). The extent to which this occurs reflects the order of cross-talk; for example, whether the neutron scatters into one detector registering an event or two thus registering two further events. Additionally, a couplet may also appear as a triplet if one of the two neutrons comprising the true couplet is scattered and detected by other detectors within the gate. For simplicity, the case where both particles in a real couplet undergo cross-talk is ignored as this is generally considered highly improbable, as subsequent analysis will show<sup>1</sup>.

Based on the assumptions described above, a correction model based on a truncated balance equation for each of the multiplets (i.e.  $F_x$ ) of an event type  $X$  (i.e. neutron or photon) follows, as expressed in Equation 1,

$$F'_x(n) = \underbrace{F_x(n)(1 + \sum_{k=1}^{\infty} XT(k))}_{\text{correction term for updraft}} - \underbrace{\sum_{m=n-k}^{\infty} (F_x(m) \sum_{k=1}^{\infty} XT(k))}_{\text{correction term for downdraft}} \quad (1)$$

where  $F'_x(n)$  is the  $n^{\text{th}}$  multiplet distribution corrected for cross-talk and  $XT$  is the empirical, arrangement-specific *cross-talk factor*: this is defined as the ratio between the number of cross-talk events to the total number of events detected as a function of order of cross-talk  $k$ ;  $n$  is the order of multiplet (i.e., singlets, couplets, triplets, etc.) and  $m = n - k$  where  $m > 0$ .

Since the radiation quanta emitted by AmLi and <sup>137</sup>Cs are not correlated in time, any pair of events recorded within the specified gatewidth for these sources constitutes cross-talk; hence the *cross-talk factor* can be estimated from such measurements. The distributions in Table 1 illustrate the *cross-talk factor* from both experiments using these uncorrelated sources and dedicated simulations for both the 8- and 15-detector arrangements. The simulations were conducted with 1 million particles in each case, representing mono-energetic neutron source of 0.75, 1, 1.25, 1.5, 1.75, 2, 2.25, 2.5, 3.5 and 5 MeV neutron and photon beams, AmLi (neutron), <sup>137</sup>Cs (photon) and <sup>252</sup>Cf (neutron) sources. The cut-off energy and gatewidth were set at 200 keVee and 25 ns, respectively, in accordance with the experiments. The results of the simulations agree with the experimental results for the 8-detector arrangement, suggesting that the formalism introduced above reflects observations consistently.

<sup>1</sup> For example, the probability of cross-talk for a 2.5 MeV neutron in the 15-detector setup is estimated at only 0.55%, as shown in Table 1.

Figure 4c illustrates the trend in cross-talk factor as a function of neutron energy for different cut-off energies for the 15-detector arrangement.

*(b) Photon breakthrough*

The emission of neutrons always has an associated  $\gamma$ -ray photon emission, and often the rate of photon emission is significantly greater. Therefore, although only a small fraction of events might be misclassified by a pulse-shape discrimination algorithm, even a small degree of bleed-through (breakthrough) by  $\gamma$ -ray photons in the range of 3-5% can constitute a significant influence on the neutron count. This is most prominent when considering a low-energy photon field, as misidentification happens primarily in the low-energy region where the photon and neutron pulse-shapes are most similar, corresponding to the zone in which the event pulse-shapes are least distinct from one another. This is depicted in the regions associated with low levels of short and long integrals in the contour and surface plots presented in Figure 5. The data for these plots were taken using the  $^{252}\text{Cf}$  source.

The effect of photon breakthrough on the coincidence distribution can manifest in different ways, as has been considered in an analogous way to that which follows on the basis of what is observed in experimental measurements [30]. For example, the singlet neutron bin might register more counts due to the misidentification of photons. Alternatively, in the event that the couplet and triplet bins gain one count more than the preceding multiplet, the bin corresponding to the preceding multiplet will have effectively lost a count relative to the hypothetical scenario that breakthrough is zero. The model presented in this work ignores the second category as, whilst not negligible, its probability is smaller than that of the first category. Hence, only the singlet bin,  $F'_x(1)$ , is corrected according to Equation 2,

$$F'_x(1) = F_x(1) - B_x \sum_{n=1}^{\infty} F_{\bar{x}}(n) \quad (2)$$

where,  $\bar{x}$  is the total number of photons detected (given the assumption in this case that the event type  $x$  on which the assay is focused is a neutron) and  $B_x$  is defined as the particle *bleed-through factor*: this is expressed as the ratio of the number  $x$  of photon events misclassified as neutrons to the total

number of photons detected,  $\bar{x}$ . The bleed-through factors were then computed by tallying all the misidentified particles and expressing this quantity as a ratio of the total counts of that particle. This can be determined analytically from the 3D surface shown in Figure 5, by dividing the area where the neutron and  $\gamma$ -ray distributions overlap into 10 smaller zones and summing the misidentified photons in each zone. A double Gaussian fit has been used for each zone.

## 5. Validation and results

### (a) *Spontaneous fission with standardized $^{252}\text{Cf}$ source*

To validate the methods described in the previous section, a  $^{252}\text{Cf}$  source (with the SF emission rate specified in Section 3) was measured with the 8- and 15-detector arrangements as per the corresponding set-ups simulated with Geant4. As the background or accidental counts are very low when using fast neutron assay [31], these events were disregarded in the calculation. Whilst the 8- and 15-detection experimental setups were found to have absolute efficiencies of  $(1.98 \pm 0.03) \%$  and  $(2.52 \pm 0.04) \%$ , respectively, Geant4 recorded  $(2.19 \pm 0.03) \%$  and  $(2.78 \pm 0.03) \%$ . This difference is perhaps due to the Geant4 simulations not taking account of the secondary photon source from decay products; hence the Geant4 depiction of the detectors had a lower dead-time, despite an approximate dead-time analysis<sup>2</sup> of the experimental data having been made.

The models have been validated using the gate fraction ( $f_g$ ) for doubles in the analytical formulation as proposed by Ensslin [32]. Since liquid scintillators detect fast neutrons with a detector prompt die-away coefficient of typically  $\sim 3.2$  ns [27], the  $f_g$  is very close to unity, i.e., 0.999, because the majority of the prompt neutrons are detected within the limit of the assigned gate (in this case 25 ns). Table 2 shows the details of the correction terms and the final  $f_g$  for the two experiments and the results of the corresponding simulations. It presents the uncorrected foreground distributions and count rates, and distributions corrected for photon breakthrough and for cross-talk. At each stage of the analysis, this coincidence distribution was converted to the reduced factorial moment distribution,

<sup>2</sup> Dead-time was estimated at 346 ns corresponding to the time necessary to process an event by the MFA during which it is insensitive to subsequent events. Therefore it is anticipated that for every detected neutron, 8- and 15-detector assays had two and three additional detectors that were busy processing  $\gamma$ -ray events, respectively.

which allows for the computation of the efficiency of the assay using the singles equation. Finally, using the doubles equation, the effective  $f_g$  was computed accordingly. Prior to applying the correction factors, the effective  $f_g$  of the 8- and 15-detector arrangements were  $0.799 \pm 0.004$  and  $0.88 \pm 0.01$ , respectively. By way of illustration, these estimates were reached by determining i) the detection efficiency via the ratio of the total number of neutron events detected to the source neutron emission rate (the latter given in section 3) and ii), the foreground distribution doublet and triplet rates in Table 2, corrected for the relative dead-time. The latter conjectured that, by definition, for doublets a detector is busy with a neutron count and for triplets two detectors are busy with a neutron count each; the influence of the  $\gamma$ -ray field was incorporated by apportioning two busy detectors to photon events for each case to reflect the higher photon field intensity but reduced interaction probability by which photons might be detected. Finally, the doubles count rate was then computed by determining the second factorial moment of the distribution. Values for the first,  $\nu_{s1}$ , and second,  $\nu_{s2}$ , factorial moments of the  $^{252}\text{Cf}$  spontaneous fission distribution of 3.76 and 11.96 were used, respectively.

First, photon breakthrough was accounted for by considering a bleed-through of 4% of photon events with a standard deviation of 1% based on 5 detectors selected at random from those constituting the arrays. Since photons are not present in the simulations, no data are included for these. The correction made to the singlet bin ( $F_n(1)$ ) results in a percentage increase in uncertainty from  $\pm 0.03$  to  $\pm 0.27$  for the 8-detector arrangement and from  $\pm 0.04$  to  $\pm 0.21$  for the 15-detector arrangement. At this stage, following the removal of the misidentified photon contribution,  $f_g$  for the two setups is  $1.19 \pm 0.01$  and  $1.20 \pm 0.01$ , respectively. These results imply that the assay is registering more neutrons than it should from the  $^{252}\text{Cf}$  source, which is consistent with a contribution due to cross-talk, which in turn increases the multiplet order, as discussed earlier. These values are consistent with the results of the simulation, as both sets of data contain cross-talk neutrons. Also, the neutron singlet count is increased by 18-24% due to photon bleed-through which impacts the analysis, as illustrated by the corresponding values for  $f_g$ .

Finally, the cross-talk factor was applied to correct the distribution for this effect, which results in a  $f_g$  of  $1.06 \pm 0.01$  and  $0.96 \pm 0.01$  for the 8- and 15-detector set-ups, respectively. This suggests that, subsequent to the correction for breakthrough and cross-talk, almost 99% of all detected

neutrons from spontaneous fission have been detected correctly in the assay. This is also confirmed by the simulation results and demonstrates that even a small contribution due to cross-talk (<1%) can increase the gate fraction  $f_g$  significantly, i.e., by 20%, while the inflations seen in couplets and triplets are estimated at between 8-12% and 30-40%, respectively.

*(b) Induced fission with  $U_3O_8$*

For a practical demonstration of the type of special nuclear material assay measurements that might be advanced by the methods described in this work, nine standardized 200 g samples of  $U_3O_8$  with the enrichments stated in Section 3 were irradiated with the same AmLi source using each of the three detector arrangements shown earlier in Figure 3. Figure 6 shows the relationships of count rates with  $^{235}U$  enrichment for singlets (left-hand axis) and couplets (right-hand axis) obtained from the experiment for all three assays: a) 8 detectors, b) 15 detectors and c) the castle. The measurements were taken for durations of approximately 2500, 1500 and 500 seconds for the 8-detector, 15-detector and castle setups, respectively. The plots were normalized to the distribution measured with an empty sample canister and the source to remove any contribution from background and AmLi. These data have not been corrected as per the models developed in this work because the photon contribution was not recorded with which to derive the photon bleed-through coefficients, and the coupling between neutron fields from AmLi and induced fission has not been included in the crosstalk model.

In the low-enrichment region, i.e., < 5 wt. %, the trend between count rate and mass approaches linearity. However, for the three larger samples (for  $^{235}U$  enrichments of  $(20.31 \pm 0.02)$ ,  $(52.80 \pm 0.04)$  and  $(93.23 \pm 0.01)$  wt. % corresponding to  $^{235}U$  masses > 30 g), a decreasing trend in fission rate is exhibited with increasing enrichment. This is consistent with the higher thermal neutron absorption cross-section for  $^{235}U$  compared to  $^{238}U$ , thus reducing the neutron flux available to stimulate fission. In practice, these trends could for example constitute calibration data to inform the characterization of  $U_3O_8$  samples of unknown isotopic composition.

## 6. Conclusion

The advantage of using the multiplicity algorithm described in this paper is that it gives the size of an event cluster and the number of clusters associated with a spontaneous fission event. When integrated over a significant number of events this information can be used to determine the multiplicity of the system. Given that this yields what is essentially a number distribution, rather than the reduced factorial moment derived in the more traditional, shift-register approach, it is potentially easier to add correction terms to the distribution to account for different physical phenomena such as self-multiplication, self-shielding, cross-talk, neutron- $\gamma$  misidentification, etc. Since the approach results in an assessment of individual clusters, each corresponding to a single fission event, the system will have an upper limit in terms of the intensity of the radiation field it can process successfully. However, since the time needed to process each cluster is  $\sim 200$  ns (40 ns if we ignore the accidental gate given the level of accidentals is very small), the testing sample will have a maximum limit of 6.7 Mfission/second.

This paper has proposed and validated a new approach to derive the correlated event composition for the assessment of fissile substances. The effects of cross-talk and photon breakthrough on the gate fraction have been determined to be approximately 20% and 50%, respectively. Similarly, the magnitude of the effect of cross-talk has been found to be approximately 0.3%, 20% and 50% for the first-, second- and third-order coincidences (singlet, couplet and triplet counts), respectively, when using the  $^{252}\text{Cf}$  source; photon breakthrough can lead to an erroneous increase of 20% in neutron counts.

Whilst these effects can constitute deleterious influences on assessments (principally safeguard applications where high levels of measurement accuracy are required), methods by which the effects of cross-talk and photon breakthrough might be corrected have been discussed based on an algorithm that relates the cluster-sizes of coincidence event data. In future, these proposed correction models, used with carefully-constructed sensitivity coefficients, may enable bias in results due to cross-talk and photon breakthrough to be minimized, as shown in this paper using the doubles gate-fraction.

Moreover, compared to the alternative analytical cross-talk models based on the factorial moment distribution [16, 17], the proposed method is straightforward and easy to compute. The distribution based on factorial moments obtained using the shift-register technique can be converted relatively easily to the cluster-size distribution enabling these correction models to be applied to it. These developments have the potential to further the use of fast neutron detection instrumentation with scintillator-based systems, particularly in nuclear safeguards.

#### Acknowledgments

R. S. acknowledges the support of Lancaster University and the Engineering and Physical Sciences Research Council (EPSRC), the UK 'DISTINCTIVE' university consortium, ([www.distinctiveconsortium.org](http://www.distinctiveconsortium.org)) and the support of the Science and Technology Facilities Council (STFC) via the UK Nuclear Data Network (<http://www.ukndn.ac.uk/>). V. A. and M. J. J. acknowledge the support the EPSRC via an overseas travel grant, EP/P008062/1. M. J. J. also acknowledges the support of the Royal Society as a Wolfson Research Merit Award holder. The apparatus used in this research is part of the UK National Nuclear Users Facility ([www.nnuf.ac.uk](http://www.nnuf.ac.uk)) supported under EPSRC grant 'ADRIANA', EP/L025671/1.

#### Author contributions

R. S., M. J. J., S. C. and C. Z. came up with the concept. R. S. developed the models, designed and built the multiplicity register and performed the simulations. R. S., V. A., S. C. and M. J. J. planned and performed the experimental measurements. All authors contributed to the writing of the manuscript.

#### Data availability

The data that support the plots within this paper and other findings of this study are available from the corresponding author upon reasonable request.

## References

- [1] J. D. Orndoff, Prompt Neutron Periods of Metal Critical Assemblies, *Nuclear Science and Engineering* 2 (1957) 450-460.
- [2] D. Reilly, N. Ensslin, H. Smith, S. Kreiner, Passive nondestructive assay of nuclear materials addendum, U.S. Nuclear Regulatory Commission, Washington, DC, LA-UR-07-1403 (2007).
- [3] N. Ensslin, W. C. Harker, M. S. Krick, D. G. Langner, M. M. Pickrell and J. E. Stewart, Application Guide to Neutron Multiplicity Counting, LA-13422-M (1998).
- [4] J. R. Wachter, E. L. Adam, and N. Ensslin, Prototype Fast Neutron Counter for the Assay of Impure Plutonium, American Nuclear Society, San Diego, California, November 29-December 4 (1987).
- [5] K. Frame, W. Clay, T. Elmont, E. Esch, P. Karpus, D. MacArthur, E. McKigney, P. Santi, M. Smith, J. Thron, R. Williams, Development of a liquid scintillator neutron multiplicity counter (LSMC), *Nucl. Inst. and Meth.* A579, (2007) 192-195.
- [6] A. Tomanin, P. Peerani, H. Tagziria, G. Janssens-Maenhout, P. Schillebeeckx, J. Paepen, A. Lavietes, R. Plenteda, N. Mascarenhas and L. Marie Cronholm, Design of a liquid scintillator-based prototype neutron coincidence counter for Nuclear Safeguards, *ESARDA Bulletin*, No. 49 (2013) 4-12.
- [7] D. L. Chichester, S. J. Thompson, M. T. Kinlaw, J. T. Johnson, J. L. Dolan, M. Flaska, S. A. Pozzi, Statistical estimation of the performance of a fast-neutron multiplicity system for nuclear material accountancy, *Nucl. Inst. and Meth.* A784 (2015) 448-454.
- [8] L. F. Nakae, G. F. Chapline, A. M. Glenn, P. L. Kerr, K. S. Kim, S. A. Ouedraogo, M. K. Prasad, S. A. Sheets, N. J. Snyderman, J. M. Verbeke and R. E. Wurtz, Recent developments in fast neutron detection and multiplicity counting with liquid scintillator, *AIP Conf. Proc.* 1412 (2011) 240-248.
- [9] A. Enqvist, M. Flaska, J. L. Dolan, D. L. Chichester, S. A. Pozzi, A combined neutron and gamma-ray multiplicity counter based on liquid scintillation detectors, *Nucl. Inst. and Meth.* A652 (2011) 48-51.
- [10] T. Murakami, J. Kasagi, H. Harada, T. Inamura, Performance of a neutron multiplicity filter composed of six liquid scintillation detectors, *Nucl. Inst. and Meth.* A241 (1985) 172-176.
- [11] J. T. Mihalcz, J. A. Mullens, J. K. Mattingly, T. E. Valentine, Physical description of nuclear materials identification system (NMIS) signatures, *Nucl. Inst. and Meth.* A450 (2000) 531-555.
- [12] M. J. Joyce, M. D. Aspinall, F. D. Cave, K. Georgopoulos and Z. Jarrah, The Design, Build and Test of a Digital Analyzer for Mixed Radiation Fields, *IEEE Trans. Nuc. Sci* 57 (5) pt. 2 (2010) 2625-2630.
- [13] J. Wang, A. Galonsky, J. J. Kruse, P. D. Zecher, F. Deák, Á. Horváth, Á. Kiss, Z. Seres, K. Ieki, Y. Iwata, Neutron cross-talk in a multi-detector system, *Nucl. Inst. and Meth.* A397, (1997) 380-390.

- [14] M. Cronqvist, B. Jonson, T. Nilsson, G. Nyman, K. Riisager, H.A. Roth, Ö. Skeppstedt, O. Tengblad, K. Wilhelmsen, Experimental determination of cross-talk between neutron detectors, *Nucl. Inst. and Meth.* A317 (1992) 273-280.
- [15] T. H. Shin, M. J. Marcath, A. DiFulvio, S. D. Clarke and S. A. Pozzi, Neutron cross-talk characterization of liquid organic scintillators, 2015 IEEE Nuclear Science Symposium and Medical Imaging Conference (NSS/MIC), San Diego, CA, 2015, 1-4.
- [16] S. Li, S. Qiu, Q. Zhang, Y. Huo, H. Lin, Fast-neutron multiplicity analysis based on liquid scintillation, *App. Rad. Isot.*, 110 (2016) 53-58.
- [17] T. H. Shin, M. Y. Hua, M. J. Marcath, D. L. Chichester, I. Pázsit, A. Di Fulvio, S. D. Clarke and S. A. Pozzi, Neutron Multiplicity Counting Moments for Fissile Mass Estimation in Scatter-Based Neutron Detection Systems, *Nucl. Sci. and Eng.* 188 (2017) 246-269.
- [18] X-5 Monte Carlo Team, MCNP – A General Monte Carlo N-Particle Transport Code, Version 5 - Volume I: Overview and Theory, Los Alamos National Laboratory, Los Alamos, NM, LA-UR-03-1987 (2008).
- [19] T. Goorley et al. Initial MCNP6 Release Overview - MCNP6 version 1.0, Los Alamos National Laboratory, Los Alamos, NM, LA-UR-13-22934 (2013).
- [20] D. E. Cullen, TART2005: A Coupled Neutron-Photon 3-D, Combinatorial Geometry, Time Dependent Monte Carlo Transport Code, Lawrence Livermore National Laboratory, Livermore, CA, UCRL-SM- 218009 (2005).
- [21] S. Agostinelli et al. Geant4—a simulation toolkit. *Nucl. Inst. and Meth.* A506 (2003) 506.
- [22] E. Padovani, S. A. Pozzi, S. D. Clarke and E. C. Miller, MCNPX-PoliMi User's Manual, C00791 MNYCP, Radiation Safety Information Computational Center, Oak Ridge National Laboratory (2012).
- [23] D. B. Pelowitz, J. W. Durkee, J. S. Elson, M. L. Fensin, M. R. James, R. C. Johns, G. W. McKinney, S. G. Mashnik, L. S. Water, T. A. Wilcox, MCNPX2.7.0 Extensions, Los Alamos National Laboratory, Los Alamos, NM, LA-UR-11-02295 (2011).
- [24] C. A. Hagmann, J. Randrup and R. L. Vogt, FREYA-a new Monte Carlo code for improved modeling of fission chains, Los Alamos National Laboratory, Los Alamos, NM, LLNL-PROC-561431 (2012).
- [25] F. Pino, L. Stevanato, D Cester, G. Nebbia, L. Sajo-Bohus, G. Viesti, The light output and the detection efficiency of the liquid scintillator EJ-309, *App. Rad. Isot.*, 89 (2014) 79-84.
- [26] A. Enqvist, C. C. Lawrence, B. M. Wiegner, S. A. Pozzi, T. N. Massey, Neutron light output response and resolution functions in EJ-309 liquid scintillation detectors, *Nucl. Inst. and Meth.* A715 (2013) 79-86.
- [27] Z. S. Hartwig and P. Gumplinger, Simulating response functions and pulse shape discrimination for organic scintillation detectors with Geant4, *Nucl. Inst. and Meth.* A737 (2014) 155-162.
- [28] M. J. Joyce, K. A. A. Gamage, M. D. Aspinall, F. D. Cave and A. Lavietes, Real-Time, Fast Neutron Coincidence Assay of Plutonium with a 4-Channel Multiplexed Analyzer and Organic Scintillators, *IEEE Trans. Nucl. Sci.* 61 (2014) 1340-1348.

- [29] B. D'Mellow, M. Aspinall, R. Mackin, M. J. Joyce and A. Peyton, Digital discrimination of neutrons and gamma-rays in liquid scintillators using pulse gradient analysis, Nucl. Inst. and Meth. A578 (2007) 191-197.
- [30] A. Enqvist, S. A. Pozzi, M. Flaska and I. Pázsit, Initial evaluation for a combined neutron and gamma ray multiplicity counter, Nucl. Inst. Meth. A621 (2010) 493-497.
- [31] R. Sarwar, V. Astromskas, C. H. Zimmerman, S. Croft and M. J. Joyce. Real-time determination of Rossi- $\alpha$  distribution, active fast neutron multiplicity, neutron angular distribution and neutron spectrum using organic liquid scintillators, IEEE Nucl. Sci. Symp. 2017, 21-28 Oct 2017, Atlanta, USA.
- [32] N. Ensslin, W. C. Harker, M. S. Krick, D. G. Langner, M. M. Pickrell, and J. E. Stewart, Application Guide to Neutron Multiplicity Counting, Los Alamos National Laboratory, Los Alamos, NM, LA-13422-M (1998).

Figure and table captions

*Figure 1: Schematic diagrams illustrating the construction of shift-register and event-triggered multiplicity distributions in this research. a) In a shift-register based system the prompt and delayed counter is incremented at each trigger event based on the number of coincident events in the corresponding gate. This produces a reduced factorial distribution. b) The approach described in this research is based on the initiation of non-overlapping prompt and delayed gates with the number of coincident events occurring in each being recorded, producing a distribution which corresponds to the size of the incoming events cluster. Hence, compared to the shift-register based algorithm, in this illustration using the same hypothetical event train in both cases, the acquisition window is activated by the 1<sup>st</sup>, 5<sup>th</sup> and 6<sup>th</sup> triggers, with the subsequent events populating the corresponding bins.*

*Figure 2: Geant4 calculations, a) optical photon yields from scintillation in response to an electron and proton as a function of energy, and b) the experimental and simulated liquid scintillator responses to  $\gamma$ -ray photons from a <sup>137</sup>Cs source.*

*Figure 3: The experimental set-ups used in this research, schematic diagrams of a) the 8-detector and b) 15-detector and c) the 12-detector, castle arrangements, and d) a photograph of the 15-detector arrangement in use.*

*Figure 4: Detector-based cross-talk dependencies and distributions based on Geant4 simulations, a) detector cross-talk probability and corresponding exponential fit for 5 MeV neutrons for different cut-off energies as a function of detector angle (rad.) relative to the position of the detector triggered by the first event, b) the distribution of response as a function of the time taken for a cross-talk event to occur (in counts per million incident particles) for the cross-talk of 1, 2, 3.5 and 5 MeV neutrons between any detectors with a cut-off of 200 keVee, and c) the relationship between the cross-talk*

factor, as defined in Section 4a, and initial incident energy of the neutron, with piecewise polynomial (spline) fits to guide the eye.

Figure 5: Pulse-shape discrimination plots of data taken with the  $^{252}\text{Cf}$  source in this research using the pulse gradient analysis technique [29], showing the well-established degradation in discrimination between neutrons and photons in the low-energy region (low values of first- and second integral) and much-improved discrimination in the high-energy region (high values), a) contour plot of first-versus-second integrals (arbitrary units corresponding to ADC channel number) and, b), a surface plot derived with the detector response as the third parameter.

Figure 6: Data arising from the active interrogation of  $\text{U}_3\text{O}_8$  samples for singlet rate and couplet rate as a function of  $^{235}\text{U}$  enrichment, equivalent to mass range of 0 to 200g  $^{235}\text{U}$  in  $\text{U}_3\text{O}_8$ , a) 8-detector, b) 15-detector and c) castle arrangements for measurements of duration 2500 s, 1500 s and 500 s, respectively. The uncertainties on the singlet and doublet data are smaller than the size of the symbols.

Table 1: Cross-talk factors for neutrons and photons in the 8 and 15-detector arrangements, calculated except where denoted 'exp.'. First-order cross-talk factors for 0.75, 1, 1.25, 1.5, 1.75, 2, 2.25, 2.5 3.5 and 5 MeV monoenergetic neutron and photon beams as well as AmLi (neutron),  $^{137}\text{Cs}$  (photon) and  $^{252}\text{Cf}$  (neutron) sources. The detector cut-off and gatewidth were set at 200 keVee and 25 ns, respectively, for both the simulations and experiments. The uncertainties were computed for a  $1\sigma$  (68 %) confidence interval.

Table 2: Detailed trends in coincidence distribution and gate fraction ( $f_g$ ). The first three orders of the foreground coincidence distributions (i.e.,  $F_n$ ) from the 8- and 15-detector arrangements with the  $^{252}\text{Cf}$  source were obtained from experiments and simulations. The photon breakthrough and the cross-talk corrections were

*applied to obtain the 'Photon-corrected' and the 'Photon and XT-corrected' foreground distributions, respectively. For each of these distributions, the doubles gate-fraction ( $f_g$ ) was computed which demonstrates the effectiveness of the two correction models. The uncertainties were computed for a  $1\sigma$  (68 %) confidence interval.*

ACCEPTED MANUSCRIPT

Figure 1a

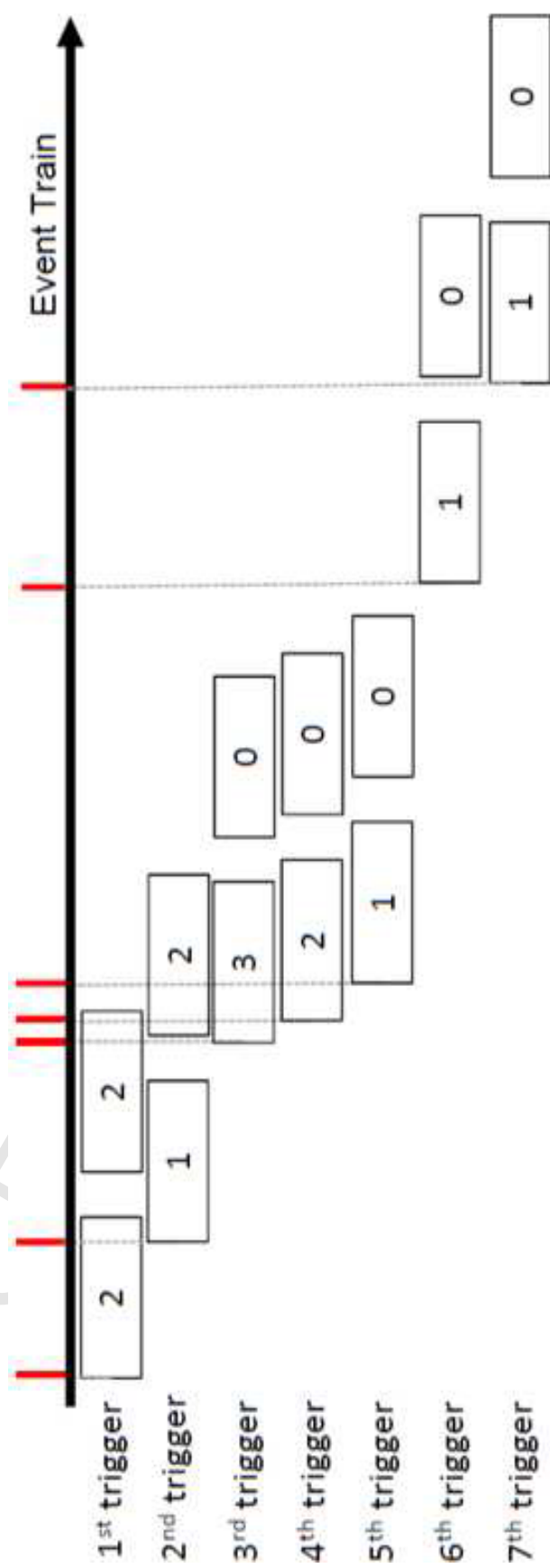
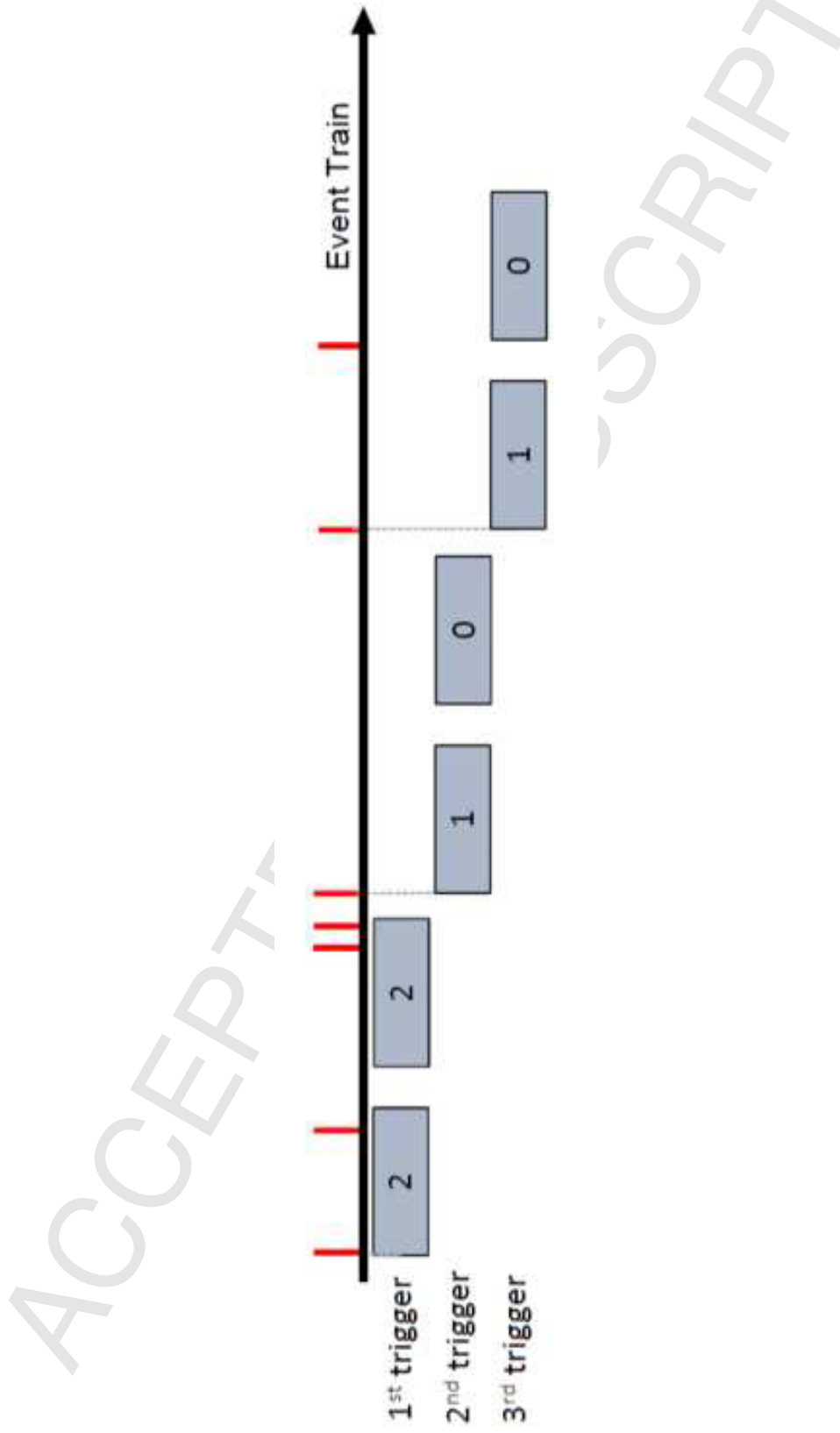


Figure 1b



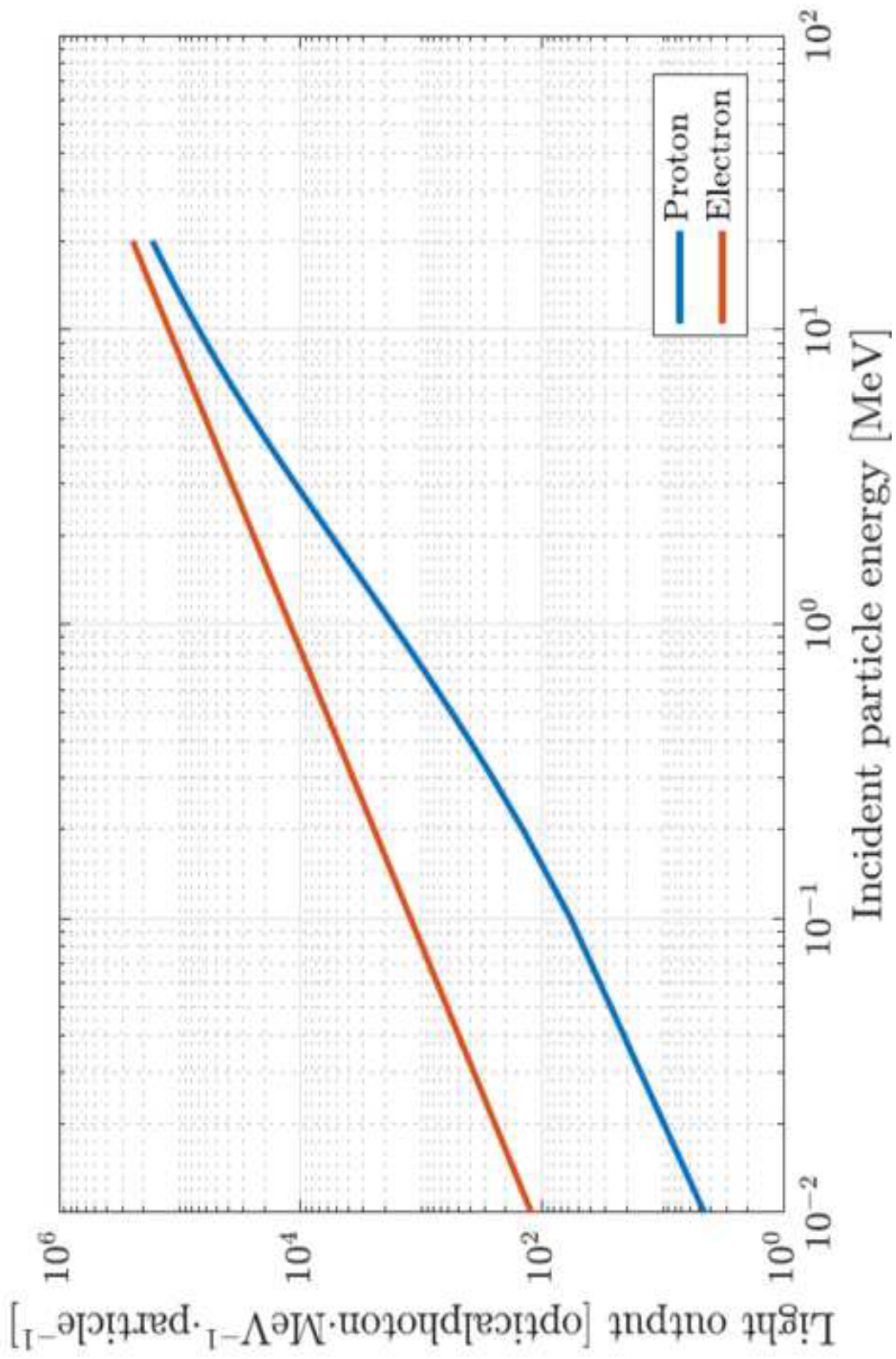


Figure 2a

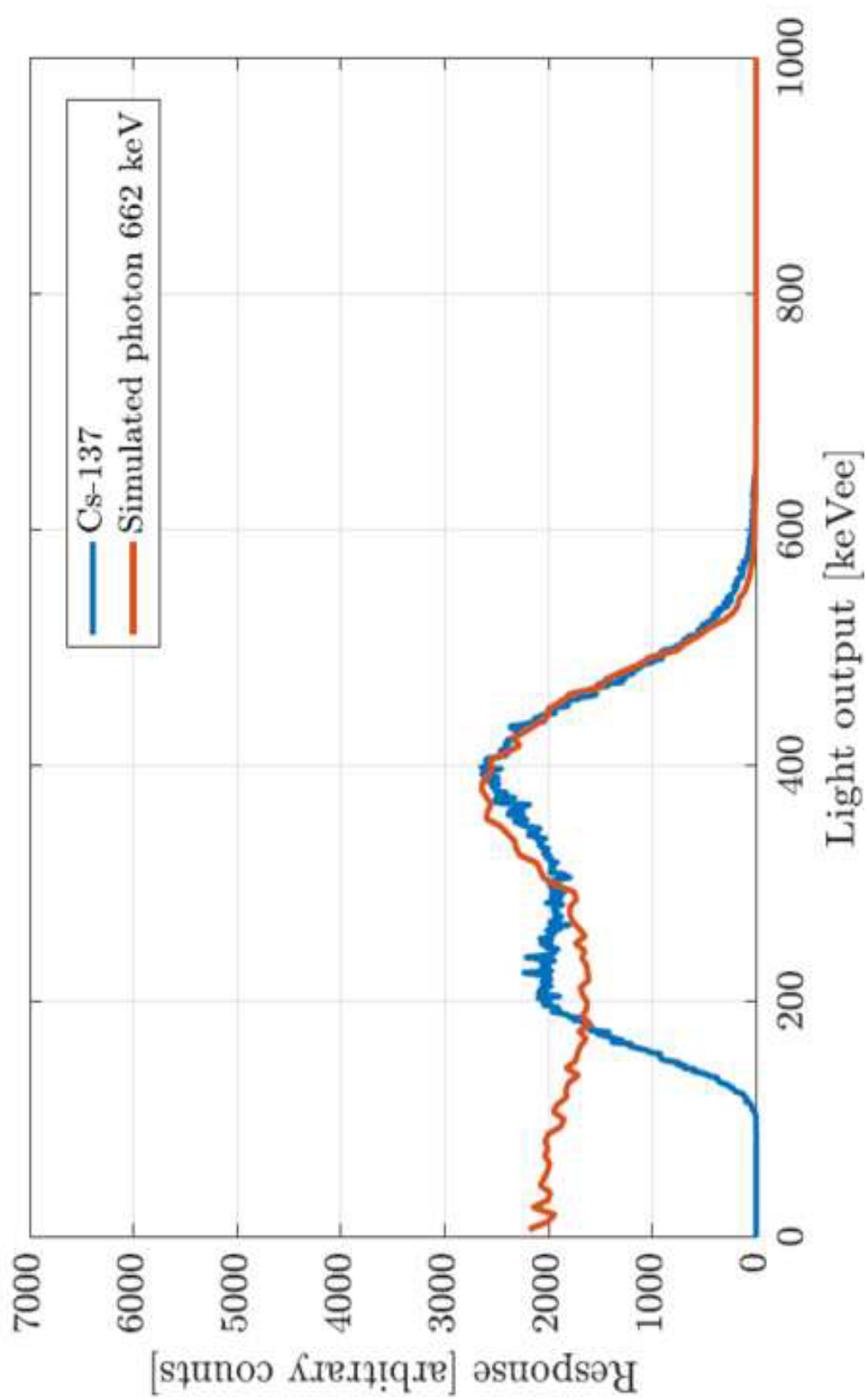


Figure 2b

Figure 3a

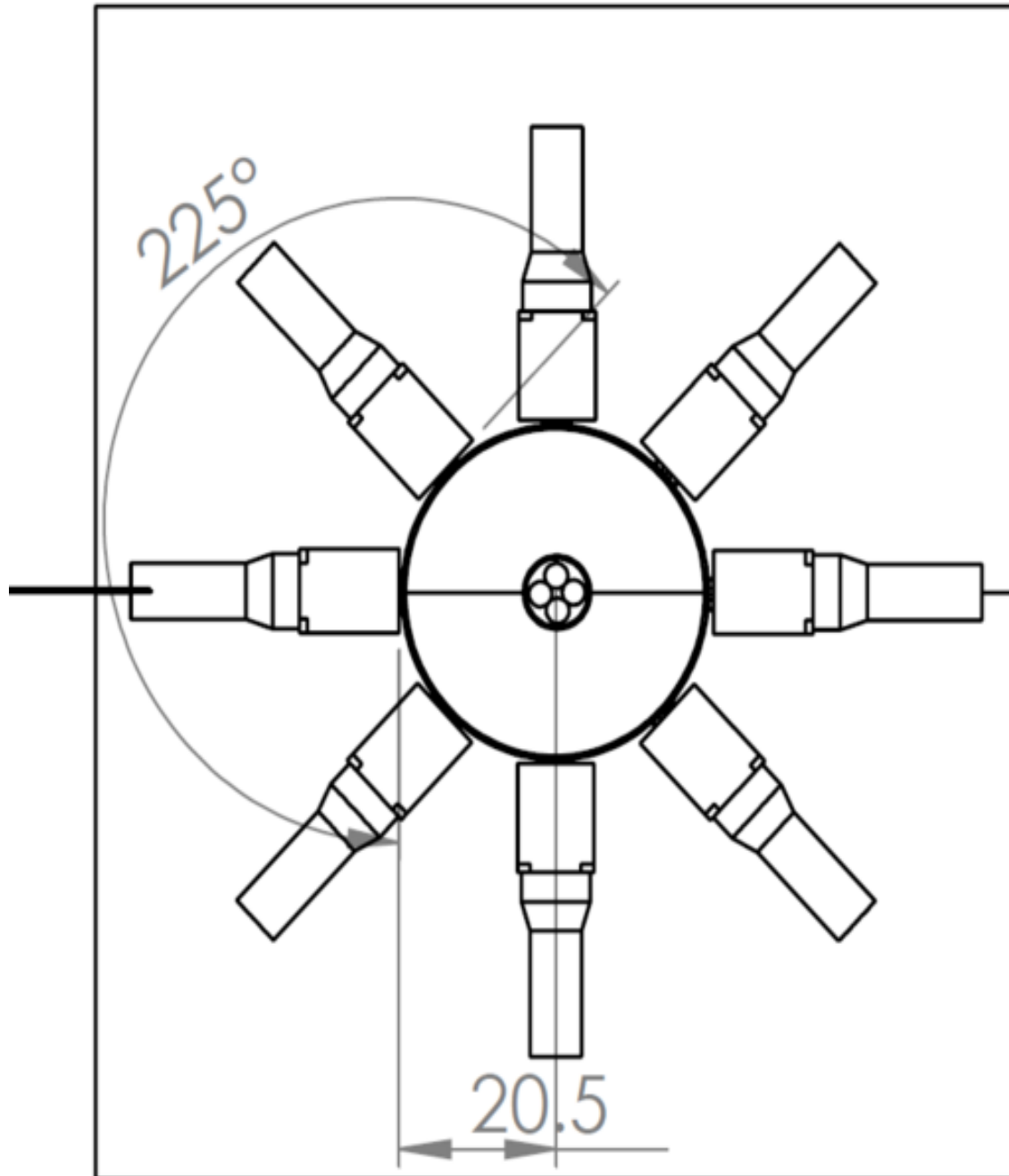


Figure 3b

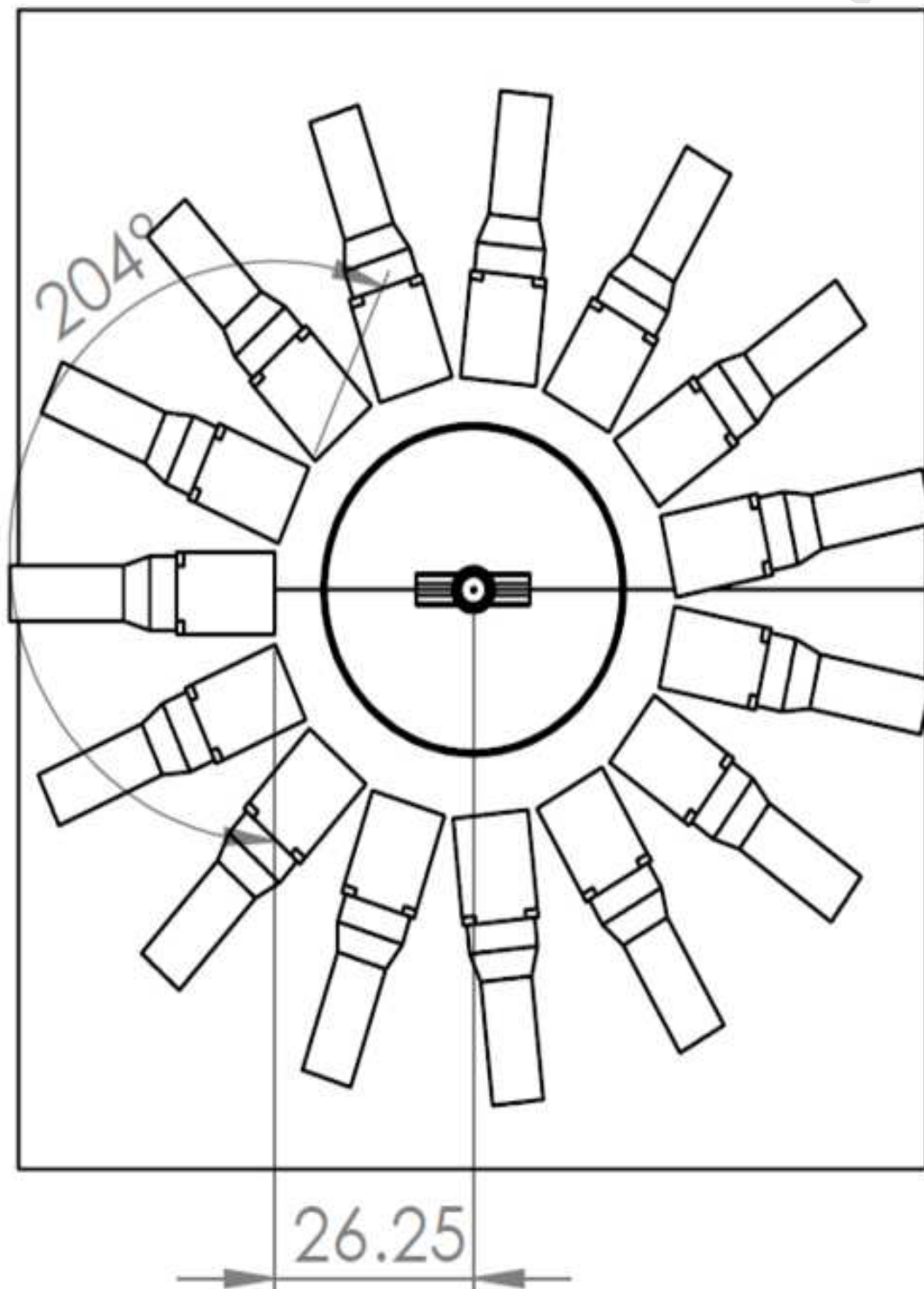
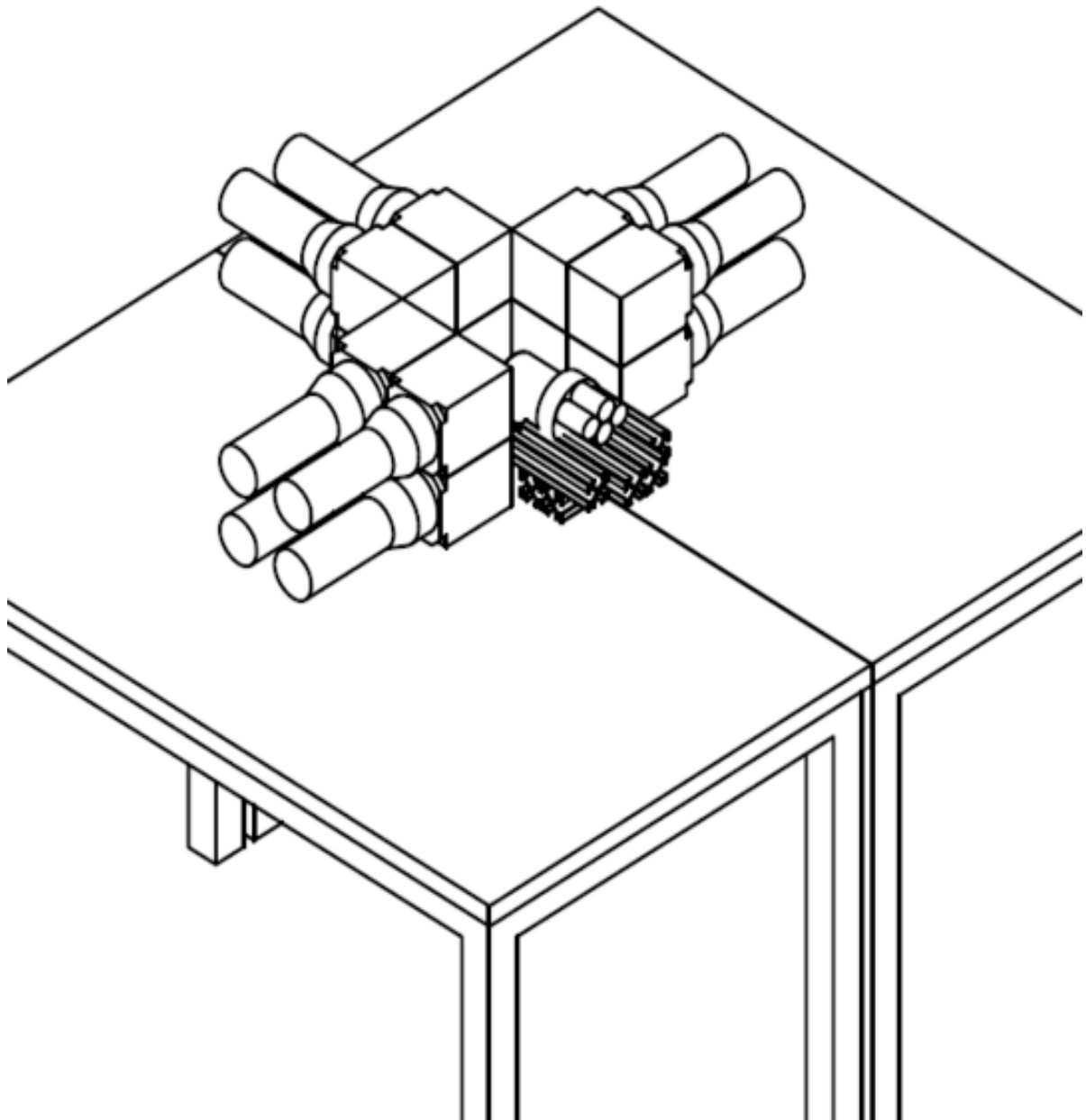


Figure 3c



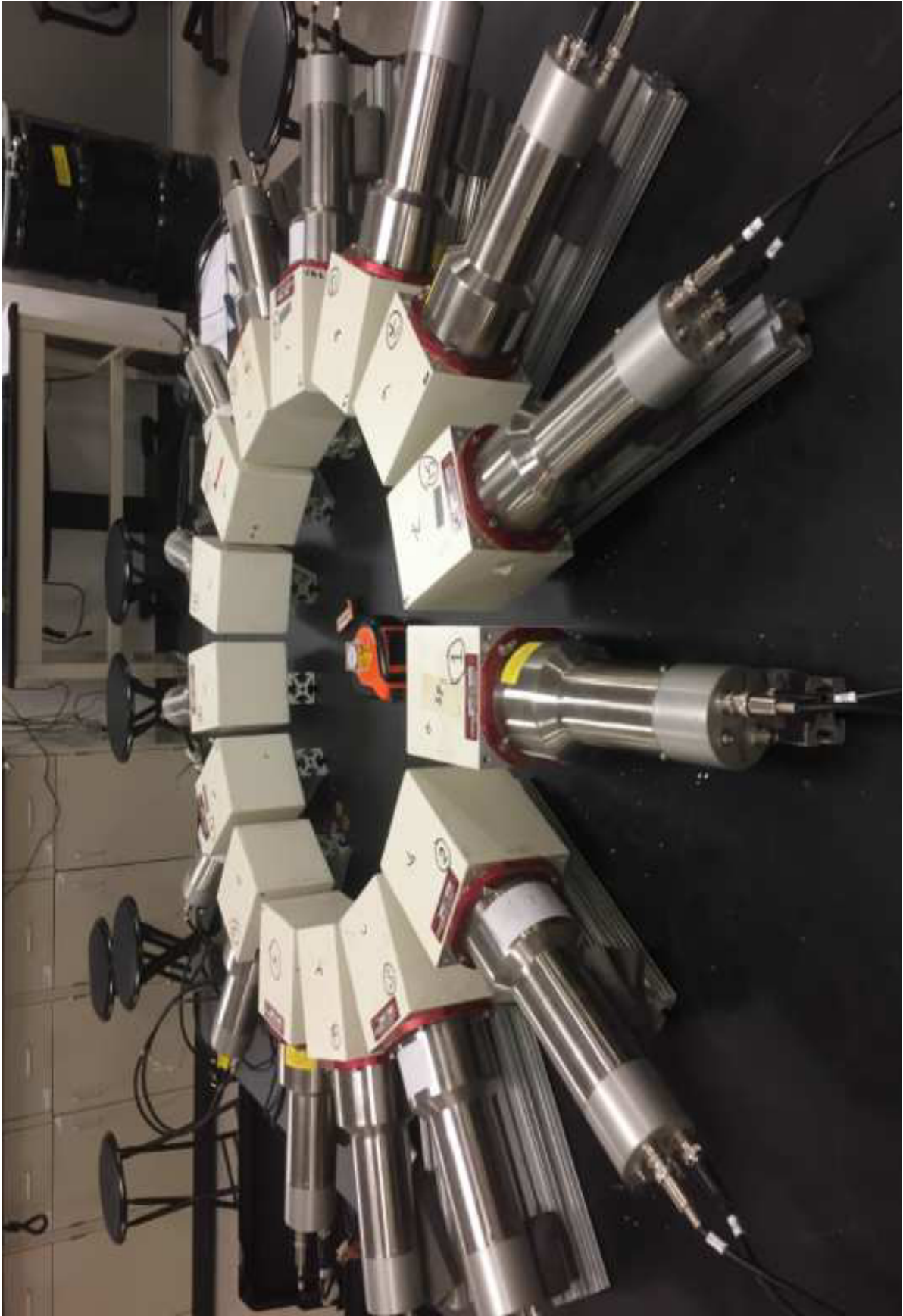


Figure 3d

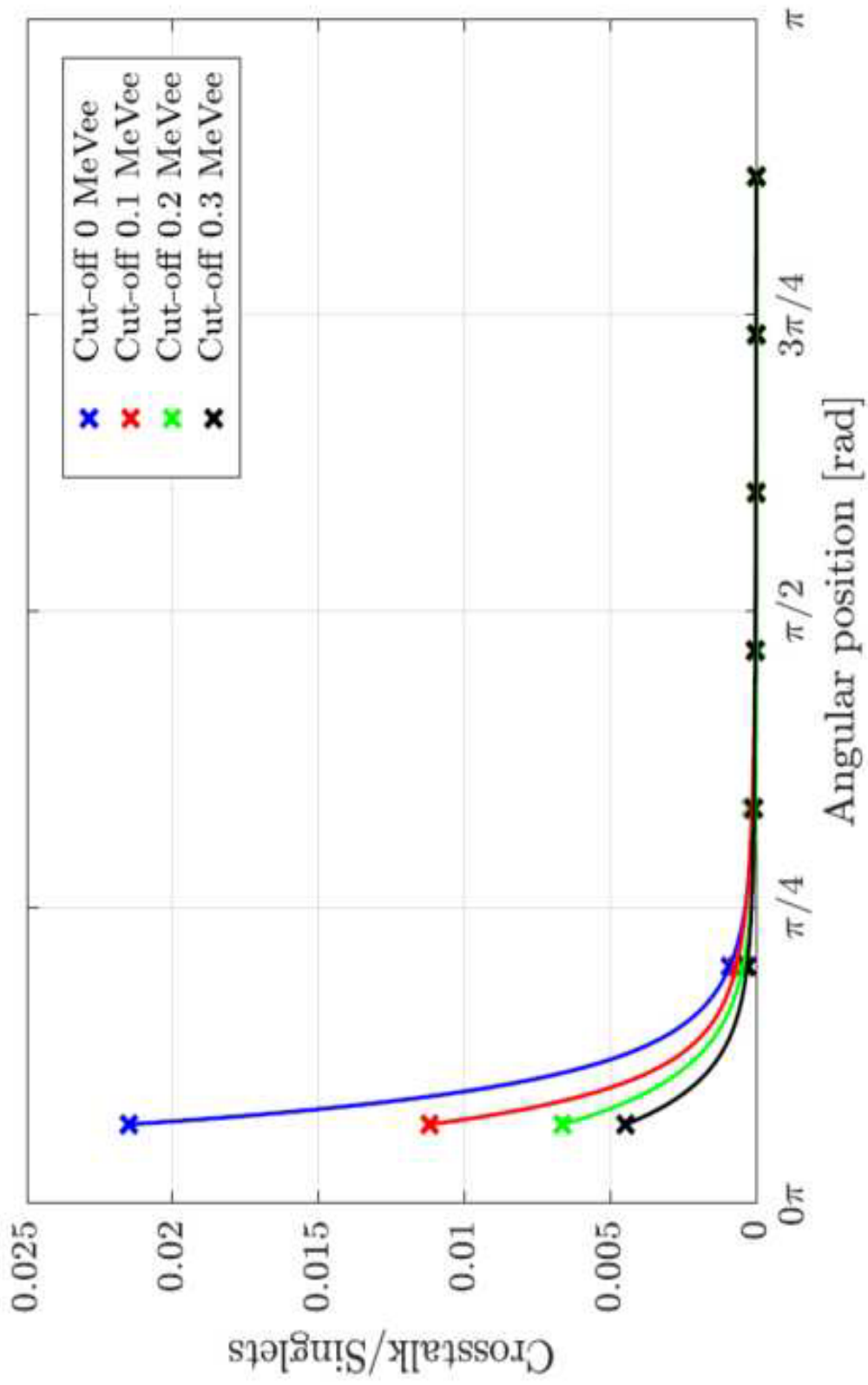


Figure 4a

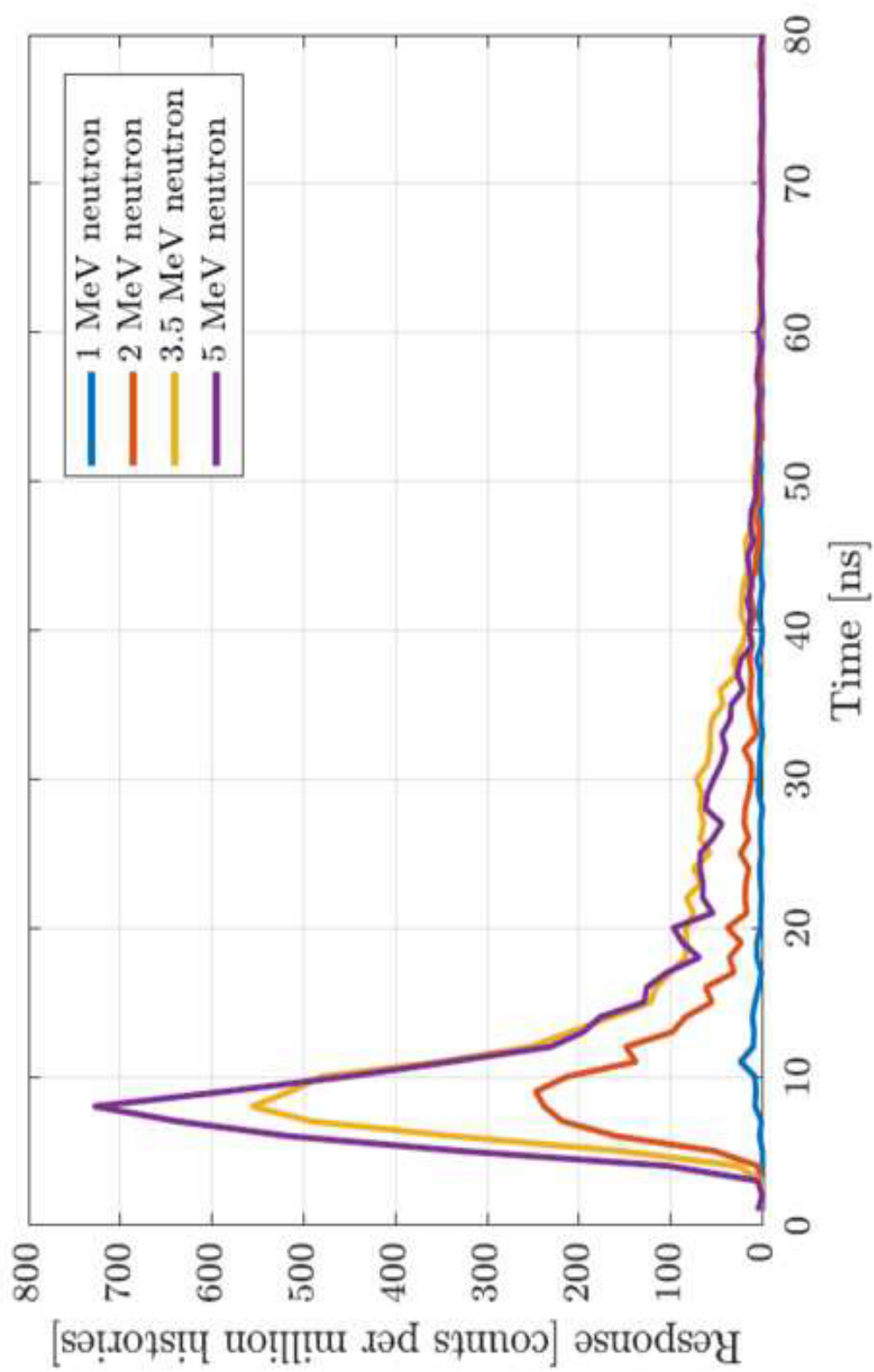


Figure 4b

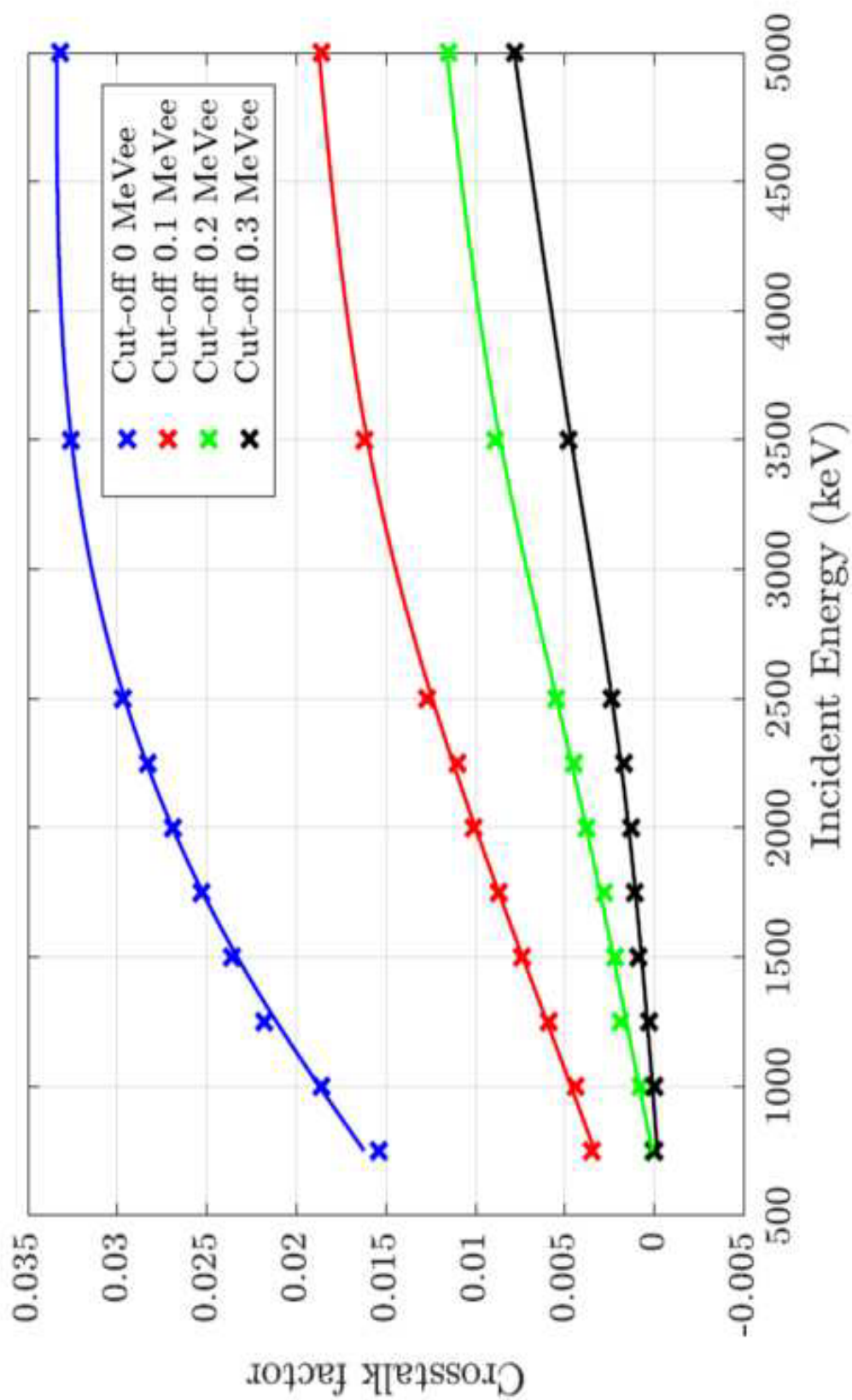


Figure 4c

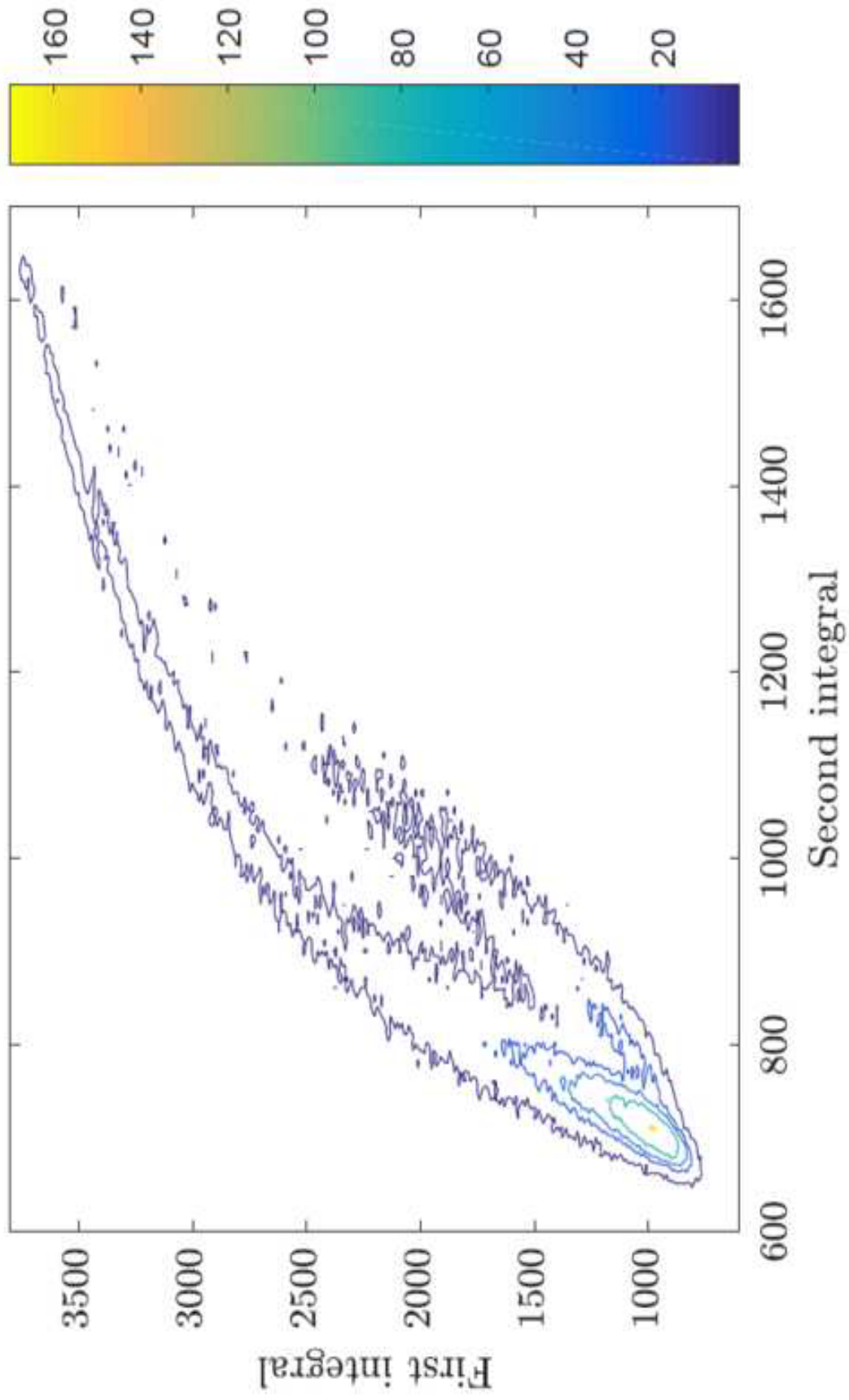


Figure 5a

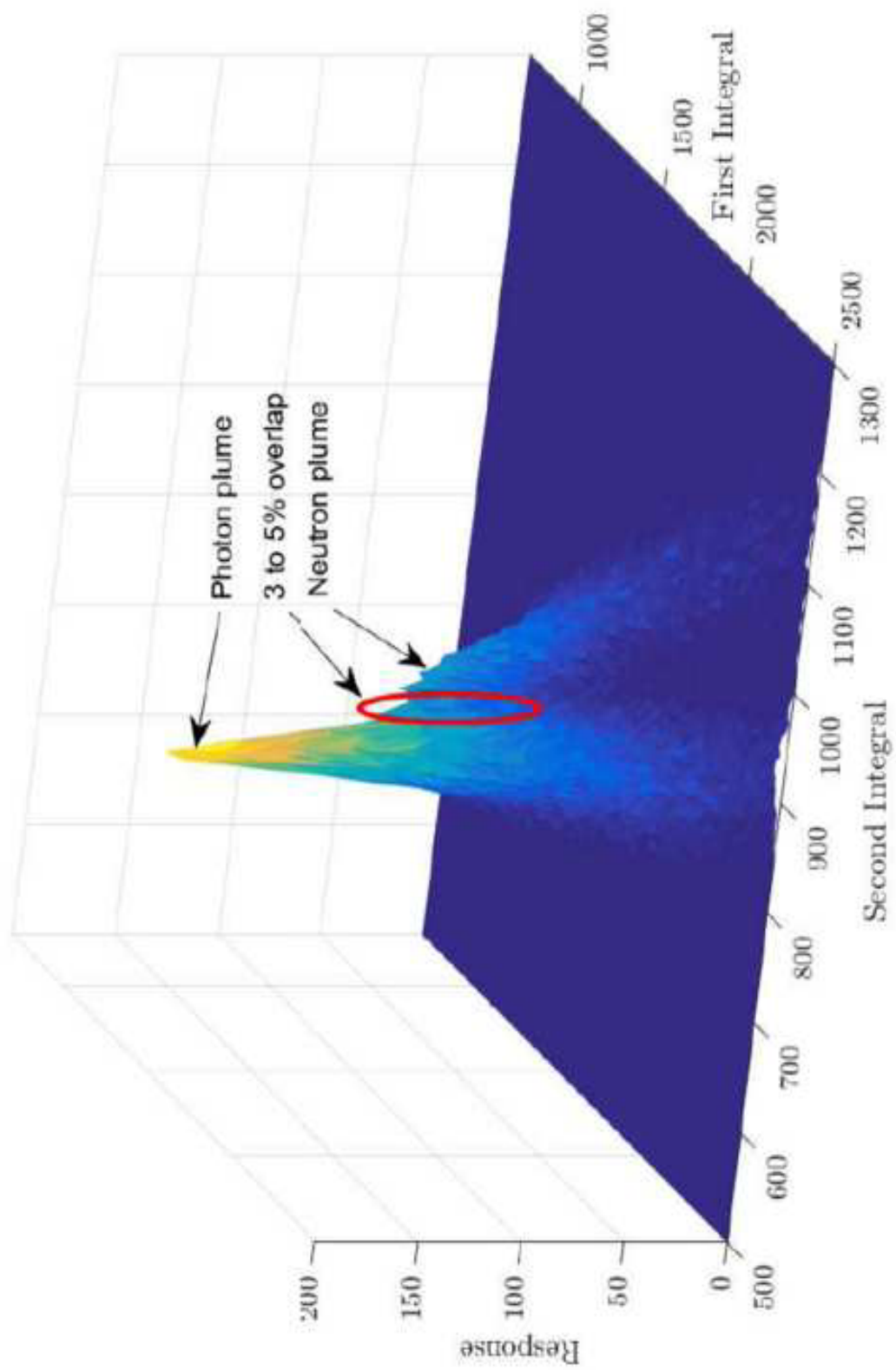


Figure 5b

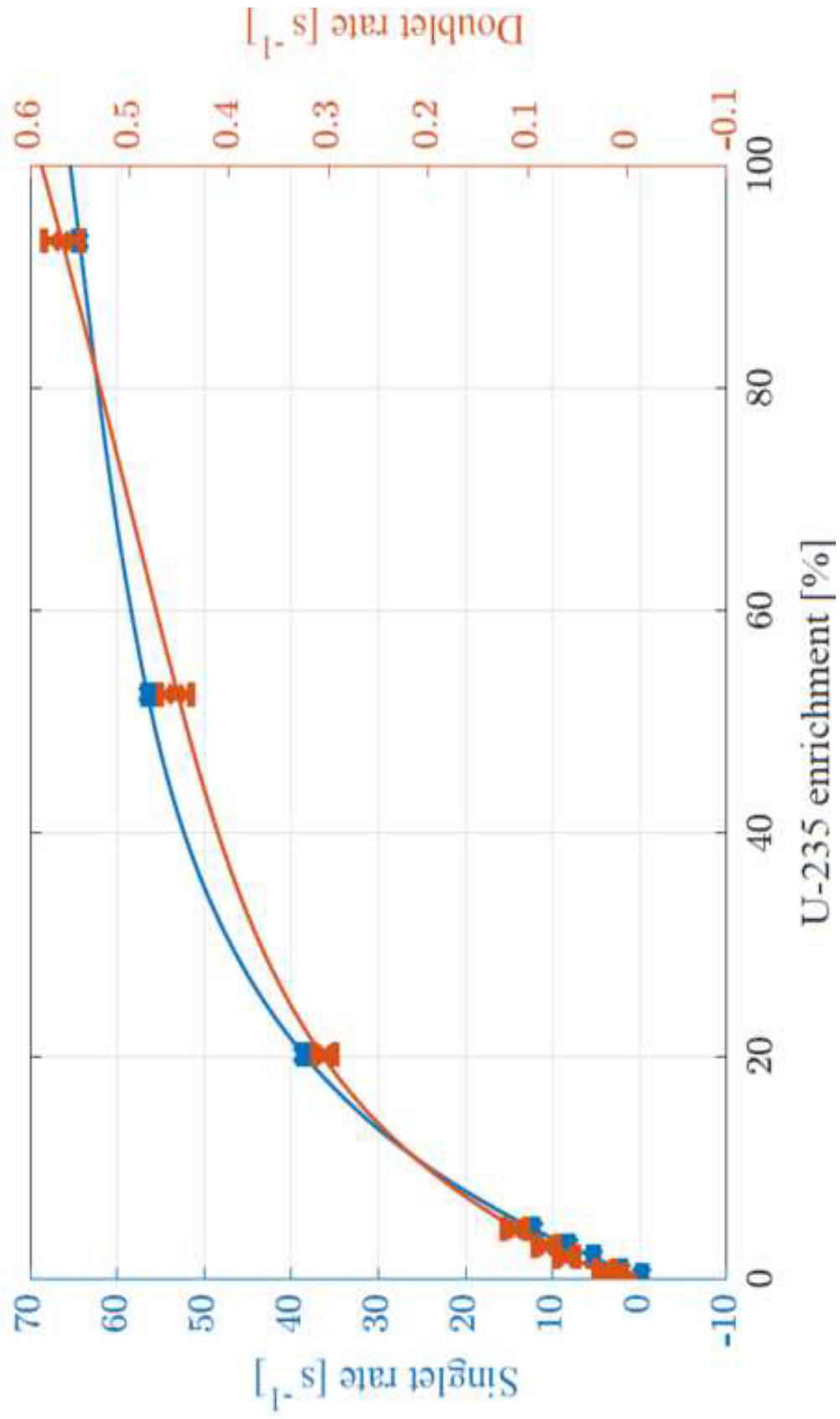


Figure 6a

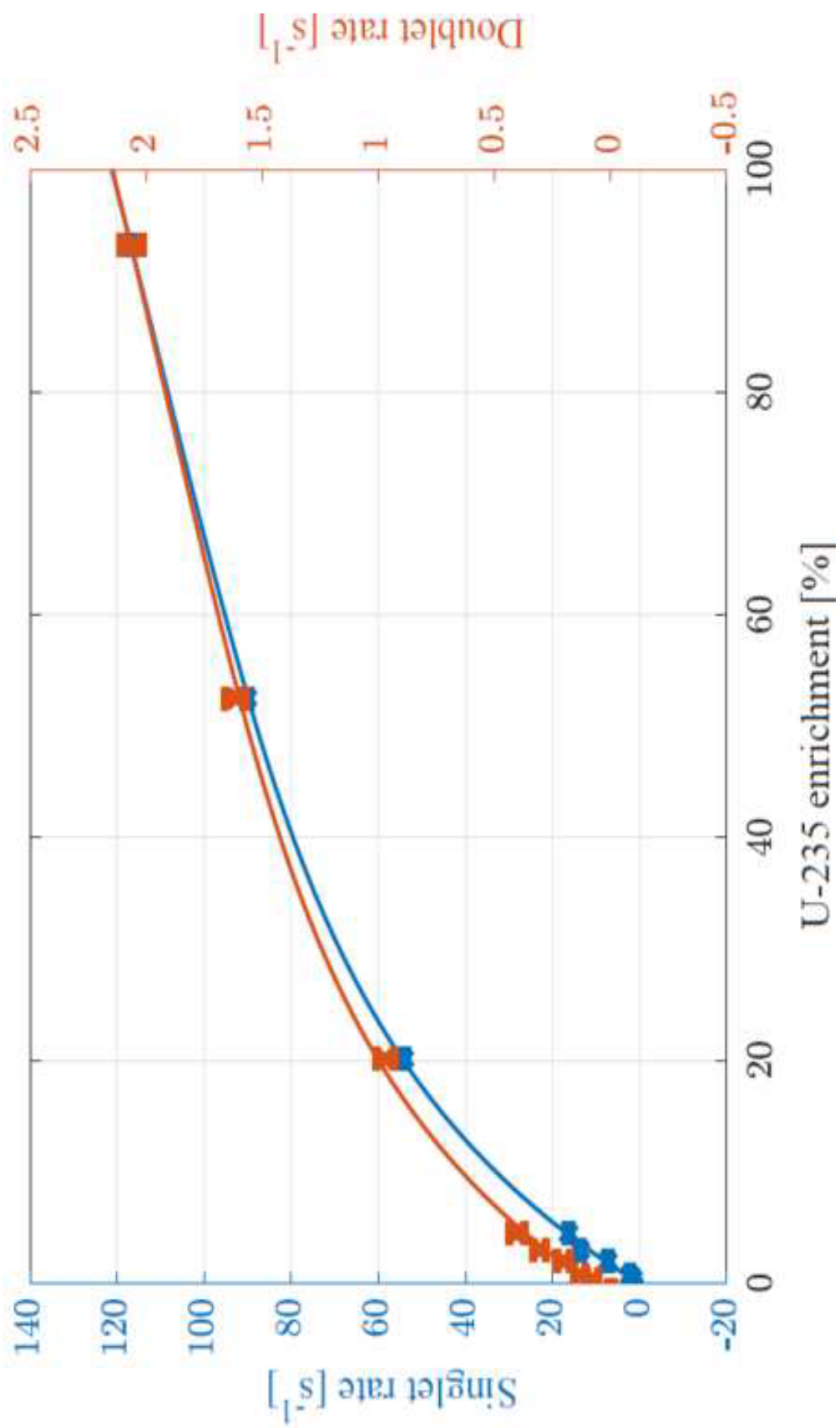


Figure 6b

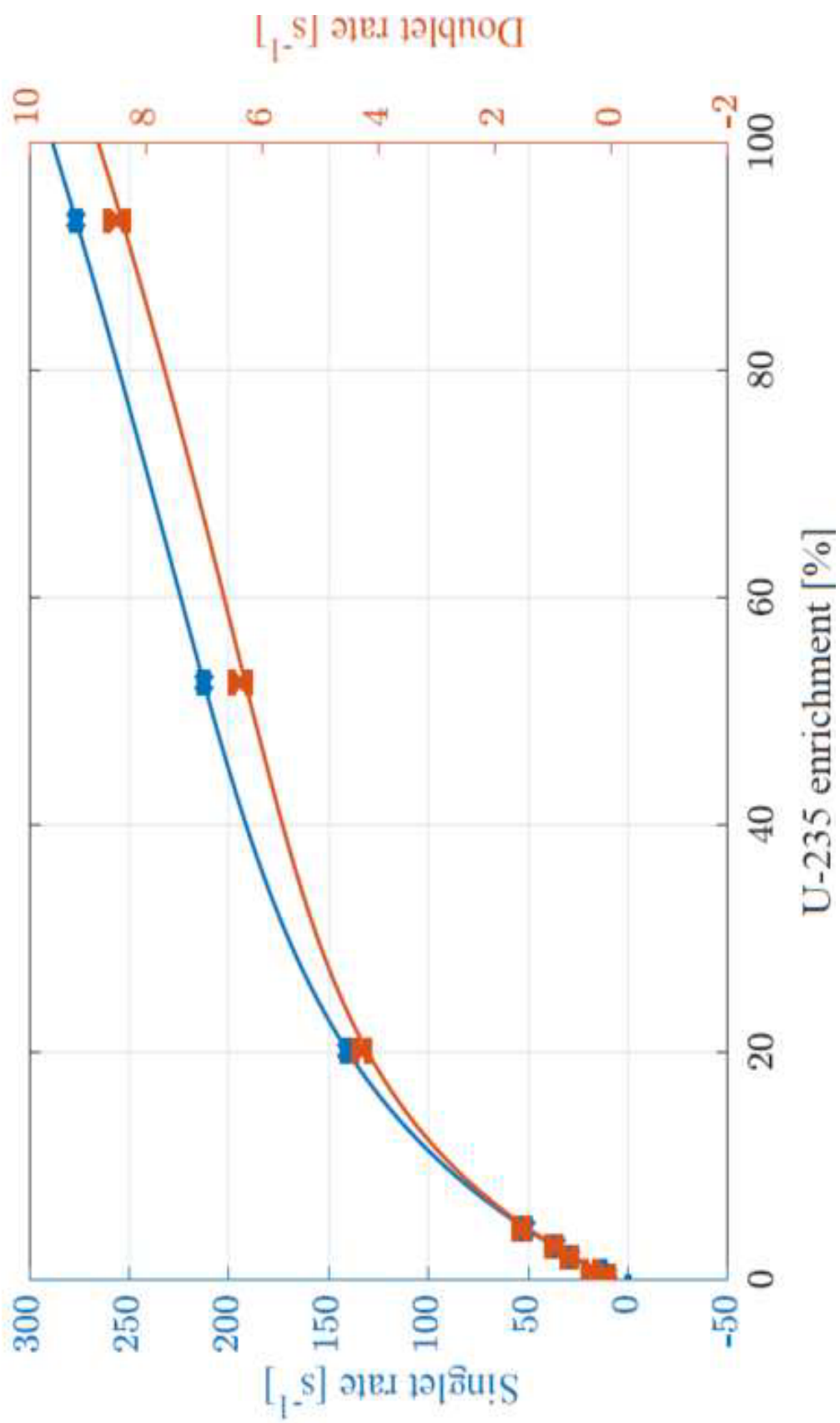


Figure 6c

Table 1

Incident Energy (keV)	Neutron		Photons	
	8-Detector	15-Detector	8-Detector	15-Detector
750	0.0000 ± 0.0000	0.0001 ± 0.0000	0.0011 ± 0.0001	0.0057 ± 0.0003
1000	0.0004 ± 0.0001	0.0008 ± 0.0001	0.0015 ± 0.0001	0.0074 ± 0.0003
1250	0.0009 ± 0.0001	0.0019 ± 0.0001	0.0022 ± 0.0001	0.0086 ± 0.0003
1500	0.0009 ± 0.0001	0.0022 ± 0.0001	0.0024 ± 0.0001	0.0091 ± 0.0003
1750	0.0011 ± 0.0001	0.0028 ± 0.0001	0.0026 ± 0.0001	0.0096 ± 0.0003
2000	0.0013 ± 0.0001	0.0038 ± 0.0001	0.0027 ± 0.0001	0.0100 ± 0.0003
2250	0.0015 ± 0.0001	0.0045 ± 0.0001	0.0029 ± 0.0001	0.0107 ± 0.0003
2500	0.0019 ± 0.0001	0.0055 ± 0.0001	0.0030 ± 0.0001	0.0108 ± 0.0003
3500	0.0034 ± 0.0001	0.0089 ± 0.0001	0.0038 ± 0.0001	0.0144 ± 0.0003
5000	0.0041 ± 0.0001	0.0115 ± 0.0002	0.0047 ± 0.0001	0.0166 ± 0.0003
AmLi <sup>1</sup>	0.0004 ± 0.0001	0.0010 ± 0.0001	Not Examined	
AmLi (exp.)	0.0016 ± 0.0001	0.0030 ± 0.0001		
<sup>252</sup> Cf	0.0025 ± 0.0001	0.0072 ± 0.0001		
<sup>137</sup> Cs (662 keV)	Not Applicable		0.0010 ± 0.0002	0.0038 ± 0.0003
<sup>137</sup> Cs (exp.)			Not Examined	0.00367 ± 0.00001

<sup>1</sup> In this case an AmLi source was simulated as a neutron source with a uniform energy distribution between 0.3 and 1.3 MeV.

Table 2

		8-detector arrangement				15-detector arrangement					
		Experiment		Simulation		Experiment		Simulation			
		Value	$f_{\underline{g}}$	Value	$f_{\underline{g}}$	Value	$f_{\underline{g}}$	Value	$f_{\underline{g}}$		
	Time (s)	1202	N/A	11.31	N/A	603	N/A	11.31	N/A		
Foreground distribution	$F_{\alpha}(1)$	$8584970 \pm 2930$	$0.799 \pm 0.004$	N/A	N/A	$5674396 \pm 2382$	$0.88 \pm 0.01$	N/A	N/A		
	$F_{\alpha}(2)$	$156696 \pm 395$				$181625 \pm 426$					
	$F_{\alpha}(3)$	$1391 \pm 37$				$2907 \pm 53$					
Foreground distribution (/sec)	$F_{\alpha}(1)$	$7142.7 \pm 2.4$	$0.799 \pm 0.004$	N/A	N/A	$9410.3 \pm 4.0$	$0.88 \pm 0.01$	N/A	N/A		
	$F_{\alpha}(2)$	$130.0 \pm 0.3$				$301.2 \pm 0.7$					
	$F_{\alpha}(3)$	$1.16 \pm 0.03$				$4.82 \pm 0.09$					
Photon-corrected foreground distribution (/sec)	$F_{\alpha}(1)$	$5770 \pm 16$	$1.19 \pm 0.01$	$6741 \pm 24$	$1.02 \pm 0.03$	$7977 \pm 17$	$1.20 \pm 0.01$	$8367 \pm 27$	$1.12 \pm 0.06$		
	$F_{\alpha}(2)$	$130.4 \pm 0.3$				$214 \pm 4$				$301.2 \pm 0.7$	$390 \pm 6$
	$F_{\alpha}(3)$	$1.16 \pm 0.03$				$2.72 \pm 0.49$				$4.82 \pm 0.09$	$11 \pm 1$
Photon and XT corrected foreground distribution (/sec)	$F_{\alpha}(1)$	$5785 \pm 16$	$1.06 \pm 0.01$	$6758 \pm 24$	$0.95 \pm 0.09$	$8034 \pm 17$	$1.00 \pm 0.01$	$8427 \pm 27$	$0.96 \pm 0.06$		
	$F_{\alpha}(2)$	$116.2 \pm 0.5$				$226 \pm 4$				$246.2 \pm 1.2$	$333 \pm 6$
	$F_{\alpha}(3)$	$0.82 \pm 0.07$				$2.18 \pm 0.51$				$2.72 \pm 0.22$	$10.5 \pm 1$

**Highlights (for review)**

- Two new models are presented to correct for the effects of cross-talk and photon breakthrough.
- The models yield consistent corrections to the corresponding gate fraction for californium-252.
- Estimates for the corresponding bias are made for the case of couplet and triplet event counts.
- A relationship is developed between the  $^{235}\text{U}$  enrichment of  $\text{U}_3\text{O}_8$  and the order of correlated, fast neutron multiplets induced by an americium-lithium source.